



Universiteit
Leiden
The Netherlands

A family tree of optical transients from narrow-line Seyfert 1 galaxies

Frederick, S.; Gezari, S.; Graham, M.J.; Sollerman, J.; Velzen, S. van; Perley, D.A.; ... ; Walters, R.

Citation

Frederick, S., Gezari, S., Graham, M. J., Sollerman, J., Velzen, S. van, Perley, D. A., ... Walters, R. (2021). A family tree of optical transients from narrow-line Seyfert 1 galaxies. *The Astrophysical Journal*, 920(1). doi:10.3847/1538-4357/ac110f















Version: Submitted Manuscript (under Review)

License: [Leiden University Non-exclusive license](#)

Downloaded from: <https://hdl.handle.net/1887/3256415>

Note: To cite this publication please use the final published version (if applicable).

A Family Tree of Optical Transients from Narrow-Line Seyfert 1 Galaxies

SARA FREDERICK ¹, SUVI GEZARI ^{1,2,3}, MATTHEW J. GRAHAM ⁴, JESPER SOLLERMAN ⁵, SJOERT VAN VELZEN ⁶, DANIEL A. PERLEY,⁷ DANIEL STERN ⁸, CHARLOTTE WARD,¹ ERICA HAMMERSTEIN ¹, TIARA HUNG ⁹, LIN YAN ¹⁰, IGOR ANDREONI ¹¹, ERIC C. BELLM ¹², DMITRY A. DUEV ⁴, MAREK KOWALSKI,^{13,14,15} ASHISH A. MAHABAL ^{11,16}, FRANK J. MASCI,¹⁷ MICHAEL MEDFORD ^{18,19}, BEN RUSHOLME,¹⁷ AND RICHARD WALTERS¹⁰

¹*Department of Astronomy, University of Maryland, College Park, MD 20742, USA*

²*Joint Space-Science Institute, University of Maryland, College Park, MD 20742, USA*

³*Space Telescope Science Institute, Baltimore, MD 21218, USA*

⁴*Division of Physics, Mathematics, and Astronomy, California Institute of Technology, Pasadena, CA 91125, USA*

⁵*The Oskar Klein Centre & Department of Astronomy, Stockholm University, AlbaNova, SE-106 91 Stockholm, Sweden*

⁶*Leiden Observatory, Leiden University, P.O. Box 9513, 2300 RA Leiden, The Netherlands*

⁷*Astrophysics Research Institute, Liverpool John Moores University, 146 Brownlow Hill, Liverpool L3 5RF, UK*

⁸*Jet Propulsion Laboratory, California Institute of Technology, 4800 Oak Grove Drive, Mail Stop 169-221, Pasadena, CA 91109, USA*

⁹*Department of Astronomy and Astrophysics, University of California, Santa Cruz, CA 95064, USA*

¹⁰*Caltech Optical Observatories, California Institute of Technology, Pasadena, CA 91125, USA*

¹¹*Division of Physics, Mathematics and Astronomy, California Institute of Technology, Pasadena, CA 91125, USA*

¹²*DIRAC Institute, Department of Astronomy, University of Washington, 3910 15th Avenue NE, Seattle, WA 98195, USA*

¹³*Deutsches Elektronen Synchrotron DESY, Platanenallee 6, 15738 Zeuthen, Germany*

¹⁴*Institut für Physik, Humboldt-Universität zu Berlin, D-12489 Berlin, Germany*

¹⁵*Columbia Astrophysics Laboratory, Columbia University in the City of New York, 550 W 120th St., New York, NY 10027, USA*

¹⁶*Center for Data Driven Discovery, California Institute of Technology, Pasadena, CA 91125, USA*

¹⁷*IPAC, California Institute of Technology, 1200 E. California Blvd, Pasadena, CA 91125, USA*

¹⁸*University of California, Berkeley, Department of Astronomy, Berkeley, CA 94720, USA*

¹⁹*Lawrence Berkeley National Laboratory, 1 Cyclotron Rd., Berkeley, CA 94720, USA*

Submitted to ApJ

ABSTRACT

The Zwicky Transient Facility (ZTF) has discovered five new events belonging to an emerging class of AGN undergoing smooth flares with large amplitudes and rapid rise times. This sample consists of several transients that were initially classified as supernovae with narrow spectral lines. However, upon closer inspection, all of the host galaxies display resolved Balmer lines characteristic of a narrow-line Seyfert 1 (NLSy1) galaxy. The transient events are long-lived, over 400 days on average. We report UV and X-ray follow-up of the flares and observe persistent UV-bright emission, with two of the five transients detected with luminous X-ray emission, ruling out a supernova interpretation. We compare the properties of this sample to previously reported flaring NLSy1 galaxies, and find that they fall into three spectroscopic categories: Transients with 1) Balmer line profiles and Fe II complexes typical of NLSy1s, 2) strong He II profiles, and 3) He II profiles including Bowen fluorescence features. The latter are members of the growing class of AGN flares attributed to enhanced accretion reported by Trakhtenbrot et al. (2019). We consider physical interpretations in the context of related transients from the literature. For example, two of the sources show high amplitude rebrightening in the optical, ruling out a simple tidal disruption event scenario for those transients. We conclude that three of the sample belong to the Trakhtenbrot et al. (2019) class, and two are TDEs in NLSy1s. We also aim to understand why NLSy1s are preferentially the sites of such rapid enhanced flaring activity.

Keywords: accretion, accretion disks — galaxies: active — galaxies: nuclei — quasars: emission lines
— relativistic processes — surveys

1. INTRODUCTION

A galaxy center hosting an active galactic nucleus (AGN) is dominated by its continuum emission. Therefore, a flare originating from this nuclear region requires a distinctly powerful event to be detectable above this stochastically variable continuum. A small number of rapid¹, smoothly evolving flares have been observed to be associated with AGN (e.g. Drake et al. 2011; Blanchard et al. 2017), with few known mechanisms that can cause these events to occur.

Intrinsic UV/optical flares, such as those due to enhanced accretion onto the central supermassive black hole (SMBH) in the form of gaseous material or stars passing too close to the nucleus, have been observed in the form of: tidal disruption events (e.g. Gezari et al. 2012; van Velzen et al. 2020a), UV-bright flaring events that are associated with accretion rate changes (Trakhtenbrot et al. 2019a), transients with double peaked line profiles linked to accretion disk emission (e.g. Halpern & Eracleous 1994), or changing-look AGN — the dramatic change in spectroscopic AGN classification following a rise in continuum level, thought to be connected to unstable changes in accretion state (e.g. LaMassa et al. 2015; Runnoe et al. 2016; MacLeod et al. 2016; Ruan et al. 2016; Stern et al. 2018; Ross et al. 2018; Trakhtenbrot et al. 2019b; Frederick et al. 2019; Graham et al. 2020).

Phenomena extrinsic to the SMBH accretion engine, such as microlensing of a quasar by a foreground Galactic source (e.g. Lawrence et al. 2012) or slowly evolving super-luminous supernova (SLSN) explosions, have also been observed to cause smooth large-amplitude flares from galaxies with AGN (Graham et al. 2017). In rare cases these can be astrometrically indistinguishable from the galactic nucleus, and therefore it becomes difficult to discern whether an explosive disruption to the accretion flow has occurred, and to differentiate this from AGN variability (Terlevich et al. 1992).

Multiwavelength approaches are required to disentangle this diverse family of observed flaring behaviors from AGN. In the golden era of time domain astronomy, even with many multichromatic instruments trained on the sky, a number of newly-discovered objects continue to defy placement into a clear-cut observational category.

In order of discovery, we present a photometric class comprised of five rapid flares with similar smooth light curve shapes occurring in a subclass of AGN observed by the Zwicky Transient Facility (ZTF) survey:

- a) ZTF19aailpwl/AT2019brs ($z = 0.37362$)
- b) ZTF19abvgxrq/AT2019pev ($z = 0.097$)
- c) ZTF19aatubsj/AT2019fdr ($z = 0.2666$)
- d) ZTF19aaiqmgl/AT2019avd ($z = 0.0296$)
- e) ZTF18abjjkeo/AT2020hle ($z = 0.103$)

In Section 2 we present the follow up of these flares. In Section 3 we compare the results of their respective multiwavelength follow up campaigns to observations of a variety of related objects found in recent years, and in Section 4 we attempt to place them into a classification scheme based on observational properties, summarized in Section 5. All transients in the sample are referred to by their ZTF alert names throughout. All magnitudes are reported in the AB system and light curves are shown in the observed frame unless otherwise stated. We have adopted the following cosmology: $H_0 = 70$ km s⁻¹ Mpc⁻¹, $\Omega_\Lambda = 0.73$ and $\Omega_M = 0.27$.

2. OBSERVATIONS

The Zwicky Transient Facility Survey (Bellm et al. 2019a; Graham et al. 2019) is comprised of the automated Palomar 48-inch Samuel Oschin Telescope (P48) as well as the Palomar 60-inch SED Machine (P60 SEDM; Blagorodnova et al. 2018; Rigault et al. 2019), and has surveyed the Northern Sky with g - and r -band filters with a 3-night cadence since 2018 (Bellm et al. 2019b). At least 15 images meeting good quality criteria were stacked to build a coadded reference image of each observing field and quadrant in each filter band. Science images are subtracted by their references and processed each night by the Infrared Processing and Analysis Center (IPAC) pipeline (Masci et al. 2019). The candidate transient alert stream (Patterson et al. 2019) is distributed by the University of Washington Kafka system, and filtered through the AGN and black holes Science Working Group’s Nuclear Transients² parameter criteria (outlined in van Velzen et al. 2019, 2020b) by the Ampel broker (Nordin et al. 2019; Soumagnac & Ofek 2018), with the GROWTH Marshal user interface utilized for the coordination of follow-up efforts (Kasliwal et al. 2019).

All 5 transients included in the sample presented here were selected based on the following criteria: large amplitude, nuclear variability ($\Delta g > 1$ mag in difference

¹ We refer to flare timescales as “rapid” when they occur on week to month timescales.

² A nuclear transient was defined as that within 0.5” of the reference galaxy center. Over 9000 nuclear transients passed this filter and were ranked during ZTF Phase I, of which 27 were TDEs, over 7% were classified as SN, and over half were AGN or candidate AGN.

imaging photometry, and within $0.5''$ of the center of the host galaxy in the reference image) with follow-up or pre-flare spectra consistent with an AGN classification. This selection was not systematic (and therefore not complete), but rather the result of ongoing intersecting and collaborative searches for changing look AGN (Frederick et al. 2019), TDEs (van Velzen et al. 2019, 2020b), and superluminous supernovae (Lunnan et al. 2019; Yan et al. 2020) relying on partial human vetting from the ZTF transient alert stream, from which this sample emerged as more examples were collected. A systematic search for NLSy1 transients in ZTF will be the focus of a future study.

2.1. Optical Photometry

All transients in the sample were detected pre-peak using ZTF difference imaging photometry. The smooth light curve shapes (with scatter $\Delta g < 0.1$ mag) of the sample are shown in Figure 1. All magnitude changes are reported in g band unless otherwise noted. An analysis of the rise times to peak are measured and reported in Section 3.1.1. We report the g -band magnitude-weighted offsets for each transient, calculated using Equation 3 in van Velzen et al. (2019). ZTF forced photometry for the sample is shown in Figure 10 of the Appendix.

ZTF19aailpwl — (RA=14:27:46.41, Dec=+29:30:38.6, J2000.0) was first detected on 2019 Feb 08 as a nuclear transient within $0''.17$ of the host galaxy center. The host galaxy displayed some variability at the < 1 mag level in the Catalina Real-Time Transient Survey (CRTS; Drake et al. 2009) from 2005 to 2013.

*ZTF19abvgxrxq*³ — (RA=04:29:22.72, Dec=+00:37:07.6, J2000.0), also known as Gaia19eby, was first detected on 2019 Sept 04 as a nuclear transient within $0''.15$ of the host galaxy center. ATLAS, Gaia, and PanSTARRs also reported observations of this source on the Transient Name Server (TNS) with discovery dates of 2019 Sep 04, 2019 Sep 13, and 2019 Sep 26, respectively. The host galaxy displayed no variability above the 0.5 mag level in CRTS.

ZTF19aatubsj — (RA= 17:09:06.86, Dec=+26:51:20.7, J2000.0) was detected on 2019 Apr 27 with a significant flux increase with respect to the reference image and with an offset from the nucleus of its host of $0''.13$. During a coverage gap in the first 40 days of the rise, ATLAS reported an intriguing “bump” feature (Smartt et al. 2019). The host galaxy displayed variability at

the 2 mag level in V-band CRTS data from 2009 to 2013 (variability which was not observed in ZTF forced photometry prior to the transient).

*ZTF19aaiqmg*l — (RA=08:23:36.77, Dec=+04:23:02.5, J2000.0), also known as eRASSt J082337+042303⁴, was detected by ZTF beginning on 2019 Feb 09 within $0''.06$ of its host galaxy. The host showed no variability in CRTS for 15 years prior to its rapid rise to peak.

ZTF18abjjkeo — (RA=11:07:42.91, Dec=+74:38:02.0, J2000.0) was detected beginning on 2020 Apr 05 within $0''.02$ of its host galaxy center. The ZTF forced photometry for this source shows no variability above the level of the galaxy for > 400 days. The host galaxy of ZTF18abjjkeo was beyond the survey limits of CRTS.

2.2. Optical Spectroscopy

All spectroscopic follow-up observations for the sample are summarized in Table 1, and each epoch is shown in Figure 11 of the Appendix. The phases of the optical follow-up spectra with respect to the features in the ZTF light curves are annotated on Figure 1. All transients in this sample have spectral characteristics of NLSy1 galaxies, i.e. strong Balmer line emission with FWHM < 2000 km s⁻¹, along with other spectral features which are highlighted below and explored in detail in Section 3.2. We reduced Palomar 60” SED Machine (P60/SEDM; Program PIs: Gezari, Sollerman, Kulkarni) spectra with *pysedm* (Rigault et al. 2019), and all other spectra with *pyraf* using standard procedures.

ZTF19aailpwl — showed a striking difference to the SDSS spectrum showing it was a NLSy1 as early as 2006 (Abolfathi et al. 2018; Rakshit et al. 2017). The follow-up Folded Low Order whYte-pupil Double-dispersed Spectrograph North (FLOYDS-N; Arcavi et al. 2019 and Lowell Discovery Telescope (LDT, formerly DCT; PI: Gezari) spectra showed a steep blue continuum and a strong He II profile with Bowen fluorescence features, indicating it became a flaring SMBH belonging to the observational class established by Trakhtenbrot et al. (2019a).

ZTF19abvgxrxq — was spectroscopically identified as a NLSy1 on 2019 Sept 15 with the Liverpool Telescope (LT; PI: Perley) SPectrograph for the Rapid Acquisition of Transients (SPRAT), based on the width of the Balmer emission lines and the strength of the [O III] $\lambda 5007$ emission line. Gezari et al. (2019) reported that the LT spectrum showed evidence for blue-shifted He II $\lambda 4686$ emission as well as N III $\lambda 4640$ emission, due to the Bowen fluorescence mechanism, placing it again in the observational subclass of the Trakhtenbrot et al.

³ ZTF19abvgxrxq passed the ZTF TDE working group’s tidal disruption event criteria, and was given the nickname “Stannis Baratheon” for ease of discussion. When it was found to be among a class of AGN-associated objects serendipitously detected by ZTF, the other sources in the class were retroactively given the names of other Game of Thrones characters in the same Great House - and collectively referred to fondly as “The Baratheons”, whose motto is, appropriately, “Ours is the Fury”.

⁴ This was the only source in the sample to be detected by the extended ROentgen Survey with an Imaging Telescope Array (eROSITA, part of the Russian-German “Spectrum-Roentgen-Gamma” (SRG) mission; Cappelluti et al. 2011), and was given the name eRASSt J082337+042303. This X-ray detection coincident with the transient’s host galaxy is described in Section 2.4.

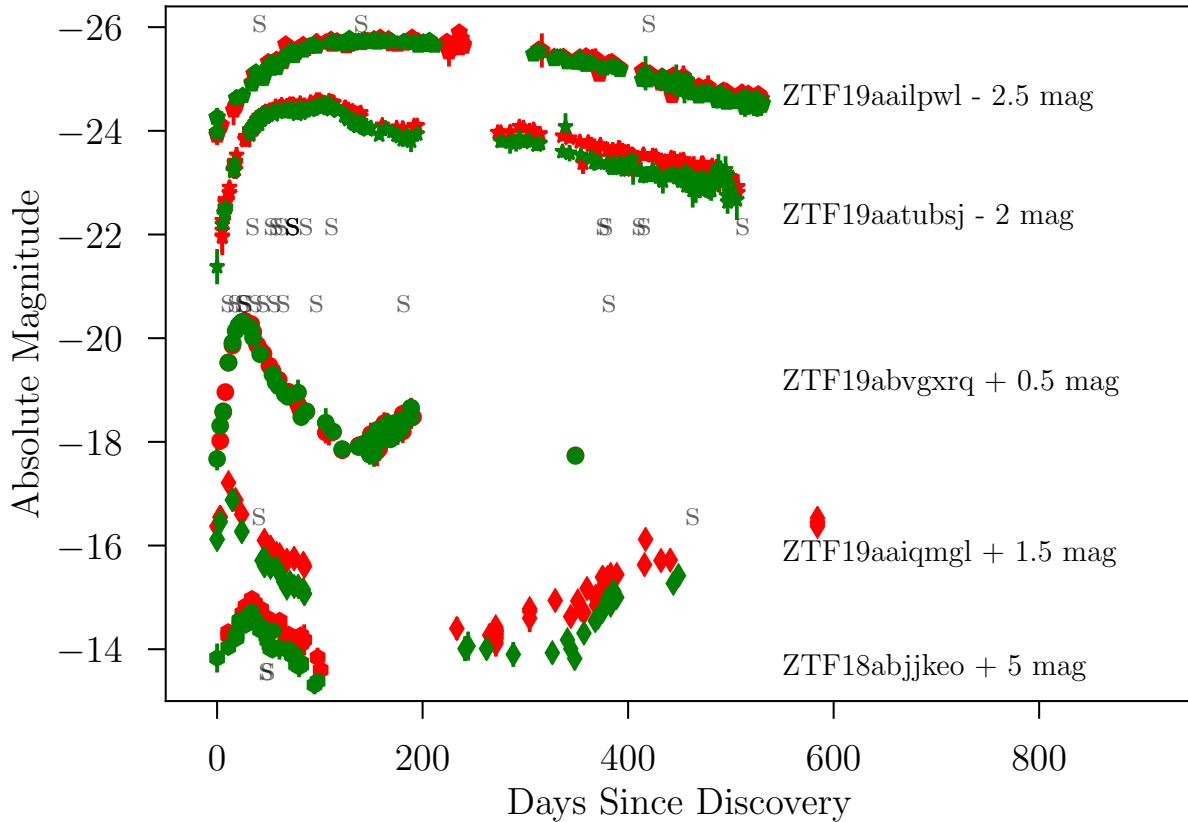


Figure 1. Comparison of the ZTF g - and r -band difference imaging light curve shapes and absolute magnitudes of the sample. ZTF19aatubsj decreases before reaching a second plateau stage, and undergoes significant reddening after the first plateau while the others never do. ZTF19abvgxqr rises again symmetrically after decreasing to pre-flare levels, as does ZTF19aaiqmgl. The light curves have been shifted in absolute magnitude space for visual purposes, as indicated alongside the object name. Overlap of the g and r light curves reflects true colors such that the initial colors approach $g - r = 0$ mag for all transients in the sample. Observations at other wavelengths are shown in Figure 2. Spectroscopic epochs are labeled for each light curve with an ‘S’ below ZTF19aatubsj and ZTF18abjjkeo and above the rest.

(2019a) objects. Near peak it was observed with Keck 10-m Low Resolution Imaging Spectrometer (LRIS; PI: Graham) as well as the LDT Deveny Spectrograph (PI: Gezari) and the KAST Double Spectrograph on the Lick 3-m Shane Telescope (PI: Foley), which confirmed the strong blue continuum and clearly defined and persistent Bowen fluorescence features.

ZTF19aatubsj — was observed 8 days after peak on 2019 Jul 03 with the Double Spectrograph (DBSP) on the Palomar 200-inch Hale Telescope (P200; PI: Yan). We measured a significant “blue horn” component of $H\beta$ and marginally detected He II. The transient continuum of ZTF19aatubsj faded to reveal an underlying Fe II complex in the Nordic Optical Telescope (NOT; PI: Sollerman) spectrum taken nearly 368 days after peak on 2020 Apr 30, with no evidence for He II emission.

ZTF19aaiqmgl — The spectrum taken with NOT (PI: Sollerman) on 2019 Mar 15 near the first optical peak

showed strong Balmer line emission, no detection of a He II line complex, and evidence for a Fe II complex, characteristic of NLSy1 galaxies. A follow-up FLOYDS-S spectrum taken 444 days after peak and reported to the Transient Name Server (TNS) by Trakhtenbrot et al. (2020) showed the appearance of He II and Bowen fluorescence features and a “blue horn” in $H\beta$. Again this event was classified as a member of the Trakhtenbrot et al. (2019a) observational class of flaring NLSy1s.

ZTF18abjjkeo — In the LT (PI: Perley) spectrum of ZTF18abjjkeo taken on 2020 May 18 8 days after peak, the narrow component of the He II profile is significantly blueshifted. No Fe II line complex was detected in the spectra of this transient.

2.3. UV Photometry

We triggered target-of-opportunity monitoring observations with the Neil Gehrels *Swift* Telescope (Gehrels

Table 1. Summary of spectroscopic follow-up observations of the sample.

Name	Obs UT	Instrument	Exposure (s)	Reference
ZTF19aailpwl	2006 Jul 01	SDSS	3000	Abolfathi et al. (2018)
	2019 Mar 15	FLOYDS-N	3600	Arcavi et al. (2019)
	2019 Jun 22	LDT Deveny	900	This work
ZTF19aatubsj	2019 May 25	Palomar 60" SEDM	2250	This work
	2019 Jun 17	LT SPRAT	900	This work
	2019 Jun 22	LDT Deveny	900	This work
	2019 Jul 03	Palomar 200" Hale	600	This work
	2020 Apr 30	NOT ALFOSC	1750	This work
ZTF19abvgxrq	2019 Sep 08	Palomar 60" SEDM	2250	This work
	2019 Sep 15	LT SPRAT	500	This work
	2019 Sep 22	Palomar 60" SEDM	2250	This work
	2019 Sep 24	LDT Deveny	600	This work
	2019 Sep 25	Keck LRIS	300	This work
	2019 Sep 25	NICER	2000	Kara et al. (2019)
	2019 Oct 01	Chandra LETG	45400	Miller et al. 2019
	2019 Oct 05	Lick 3-m KAST	1500	This work
	2019 Oct 12	LT SPRAT	500	This work
	2019 Oct 15	Chandra LETG	91000	Mathur et al. 2019
	2019 Oct 23	LDT Deveny	900	This work
	2019 Nov 01	Palomar 60" SEDM	2250	This work
	2019 Dec 03	LDT Deveny	2400	This work
2020 Feb 26	LDT Deveny	2600	This work	
2020 Jan 30	<i>Swift XRT</i>	94700	This work	
ZTF19aaiqmgl	2020 Mar 15	NOT ALFOSC	1800	Malyali et al. 2020, in prep.
	2020 Apr 28	eROSITA SRG	140	Malyali et al. 2020, in prep.
	2020 May 10	FLOYDS-S	3600	Trakhtenbrot et al. (2020)
ZTF18abjjkeo	2020 May 16	Palomar 60" SEDM	2250	This work
	2020 May 18	LT SPRAT	1000	This work

[et al. 2004](#)) for all transients in the sample. Using the HEASOFT command `uvotsource` we extracted *UVOT* photometry within a $5''$ -radius circular aperture and using an annular background region centered on the coordinates of the optical transient.

Figure 2 shows the νL_ν light curves of all flares in the sample. We compare ZTF g and r band difference imaging, WISE difference imaging, *Swift XRT* monitoring, and *Swift UVOT* detections subtracted by the archival *Galaxy Evolution Explorer* (*GALEX*; [Bianchi et al. 2017](#)) All-Sky Imaging Survey (AIS) near-UV (NUV, $\lambda_{\text{eff}} = 2310 \text{ \AA}$) host measurements (measured with a $6''$ -radius aperture).

We found all transients in the sample to be UV-bright, but with varying UV colors. The UV color of ZTF19aaiqmgl ($UVW1 - g = -0.2$ mag) was similar to that of ZTF19abvgxrq ($UVW2 - g = -0.2$ mag)

and ZTF19aailpwl (ranging from $UVW2 - g = -0.1$ mag to -0.7 mag in 80 days), but ZTF19aatubsj was the only transient in the sample with positive UV color ($UVW2 - g = 0.8$ mag). The UV light curves of the sample tend to follow the shape of the optical. ZTF19abvgxrq became host dominated over time as the transient faded. but with strong scatter in the light curve as it approached the host magnitude.

2.4. X-rays

We found only two transients in the sample to be X-ray bright in follow-up *Swift XRT* observations: ZTF19abvgxrq and ZTF19aaiqmgl. ZTF19aailpwl was detected only once, and then only at a low level. We measured an *XRT* upper limit of $0.004 \text{ counts s}^{-1}$ for ZTF19aatubsj. X-ray follow-up spectra are reported in Table 1. *Swift* photometry compared to WISE W1- and

W2-band and ZTF g and r -band photometry is shown in Figure 2. The X-ray bright flares in this sample tend to vary in lockstep with the slow UV/optical flares.

ZTF19aailpwl — was detected only once in 11 observations during a 16-month monitoring campaign between 2019 Mar 21 and 2020 Jul 7. We measured a $3\text{-}\sigma$ detection of $0.003\text{ counts s}^{-1}$ on 18 Apr 2019, just brighter than the limiting flux.

ZTF19abvgxrq — Similar to the UV light curve, the shape of the X-ray flare of *ZTF19abvgxrq* followed the optical, from its fade through its second rise (See Figure 2 and Section 3). The unabsorbed $0.3\text{--}10\text{ keV}$ flux from the stacked *XRT* spectrum of *ZTF19abvgxrq* was $7.3 \pm 0.1 \times 10^{-12}\text{ erg cm}^{-2}\text{ s}^{-1}$. *ZTF19abvgxrq* was previously detected in ROSAT, and NICER observations show an increase in flux from this by 100 times ($1 \times 10^{-11}\text{ erg cm}^{-2}\text{ s}^{-1}$), variable from 11 to 14 counts s^{-1} in 3 hours (Kara et al. 2019). A 50 ks Chandra LETG grating observation taken just 8 days after peak and reported by Miller et al. (2019) found a flux consistent with this, with the spectral shape a good fit to a $kT = 0.24\text{ keV}$ blackbody, and the source variable at the 25% level on 2–3 ks timescales. Mathur et al. (2019) reported a decrease in $0.3\text{--}2.5\text{ keV}$ flux to $7.7 \times 10^{-12}\text{ erg cm}^{-2}\text{ s}^{-1}$; their 91 ks Chandra LETG observation was a good fit to a consistent blackbody model and a power law component typical of AGN with spectral index $\Gamma = 1.8$, with no intrinsic absorption required.

ZTF19aaiqmgl — was observed only during the second optical flare (on 2020 Apr 28, 350 days after the first ZTF detection), and was the only X-ray bright transient in the sample with much fainter X-ray νL_ν than that of the optical (shown in Figure 2). Like *ZTF19abvgxrq*, the shape of the X-ray rise followed that of the second rise. It was detected by eROSITA as eRASSt J082337+042303, a soft X-ray transient consistent with the galaxy 2MASX J08233674+0423027 (Malyali et al. 2020, Malyali et al. 2020, in prep.) Prior to this, the XMM Slew Survey reported a non-detection at the location of the host galaxy, with an upper limit of $< 1.7 \times 10^{-14}\text{ erg s}^{-1}\text{ cm}^{-2}$ assuming $kT_{\text{bb}} = 100\text{ eV}$ and $N_H = 3 \times 10^{20}\text{ cm}^{-2}$. The SRG flux of $1.5 \times 10^{-12}\text{ erg s}^{-1}\text{ cm}^{-2}$ was 90 times brighter than this upper limit. No hard X-ray component was detected above 2.3 keV. No strong short-term variability on hours-long timescales was detected, and no strong variability was detected between SRG and the 3 *Swift XRT* monitoring observations taken afterward with a week-long cadence. Swift and NICER observations over the next 5 months showed an additional increase in X-ray flux by a factor of 10 (Pasham et al. 2020). A careful study of the X-ray properties of this transient is forthcoming (Malyali et al. 2020, in prep.)

2.5. IR

Malyali et al. (2020) reported that the WISE color of *ZTF19aaiqmgl* was atypically low ($W1 - W2 \simeq 0.07$

mag) compared to typical AGN values ($W1 - W2 = 0.7\text{--}0.8\text{ mag}$, Stern et al. 2012; Assef et al. 2013). The WISE colors of *ZTF18abjjkeo* (neoWISE: 0.35 mag, AllWISE: 0.036 mag) and *ZTF19abvgxrq* ($W1 - W2 = 0.45\text{ mag}$) are also inconsistent with an AGN, though not quite as low as that of *ZTF19aaiqmgl*. Only *ZTF19aailpwl* truly appeared as an AGN in IR, with $W1 - W2 = 0.98\text{ mag}$. The WISE AGN classification of the sample is summarized in Table 3 in Section 4.

A flare in the IR was detected in NeoWISE at the location of *ZTF19aaiqmgl* and concurrent with the optical and X-ray transient. Though the IR flare began much sooner in 2009, Figure 2 shows that the peak of the flare was delayed with respect to the first optical peak. Prior to this flare, WISE photometry detected no variability at the location of *ZTF19aaiqmgl* for nearly 5 years.

3. ANALYSIS

3.1. Photometry

The difference imaging light curves for the sample are shown in terms of absolute magnitudes in Figure 3.

We show the sample alongside various NLSy1-related events from the literature, which are described in more detail in Section 4. CSS100217 displayed some variability prior to the transient, unlike any of the events in this sample. AT2017bgt was observed only during its fade in difference imaging, so we instead show its aperture photometry (from the ASAS-SN Photometry Database⁵; Jayasinghe et al. 2019) which also shows the rise of the source. *ZTF18aajupnt* is by far the least luminous transient shown. We note the similarity of the shapes of the light curves of *ZTF19aatubsj* and PS16dtm, which is discussed further in Section 4.

3.1.1. Light Curve Timescales

We measured the rise-to-peak timescales of the sample by fitting Gaussians to the light curves shown in Figure 3 using the `lmfit` package. We observe a correlation between the luminosity (specifically the absolute magnitudes M_V and M_g) and rise-to-peak timescales of the sample (t_{rise}) with the following relation: $M = -0.04t_{\text{rise}} - 18.59$, shown in Figure 4. Fitting the light curves with quadratic functions resulted in the same correlation within the error estimates. Interestingly, TDEs also show a positive correlation between rise time to peak and luminosity (van Velzen et al. 2020b). *ZTF18aajupnt* appears under-luminous for how fast it rises. AT2017bgt was observed only during its fading phase in difference imaging, and so was excluded from this portion of the analysis.

3.1.2. Rebrightening

⁵ <https://asas-sn.osu.edu/photometry>

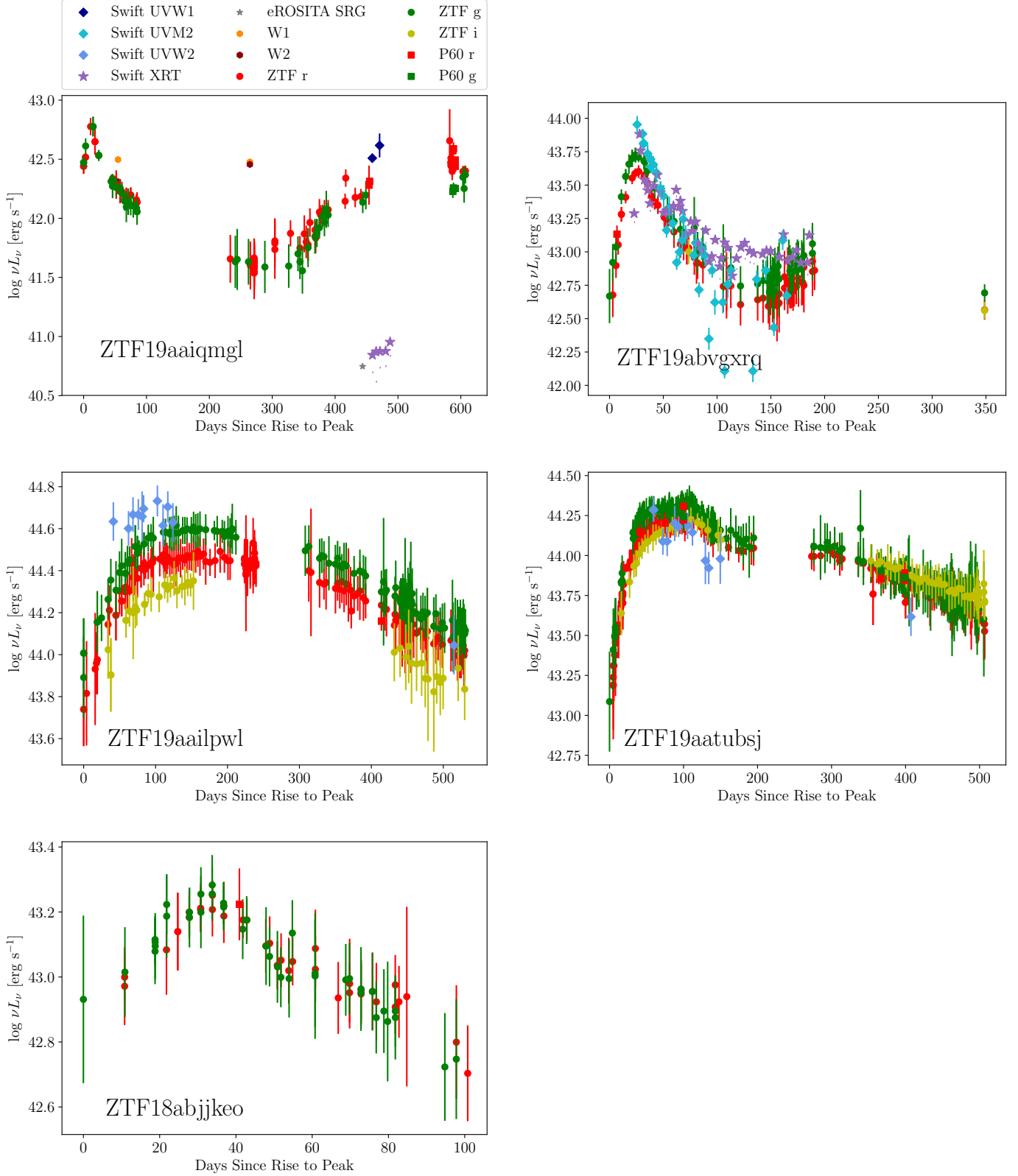


Figure 2. We track the colors of the transients in the sample with a νL_ν light curve, comparing the ZTF and WISE data to concurrent high cadence *Swift* *UVOT* and *XRT* monitoring observations. The X-ray rise and fade of ZTF19abvgxrq tracks the optical/UV with no significant delay. We subtracted the host galaxy light as estimated by *GALEX* NUV measurements from the *Swift* *UVOT* observations. Times are given in days since first ZTF detection. The X-ray errorbars are comparable to the size of the data points. See Figure 10 for pre-outburst forced photometry.

It is notable that two sources in the sample, ZTF19abvgxrx and ZTF19aaiqmg1, each have a dramatic rebrightening episode. Following a flare and an approximately ~ 2 mag fade from peak, both return to nearly half their maximum luminosity before seasonal gaps in visibility. This is in contrast to that of almost all TDEs and SN in the literature (e.g. Sollerman et al. 2019, 2020), although they can show plateaus and “humps” (e.g. Hammerstein et al. 2020, in prep.)⁶ We explore possible interpretations of this rebrightening in Section 4.

3.1.3. UV/Optical to X-ray Ratio

We derive the simultaneous UV/optical-to-X-ray spectral slope ratio (α_{OX}) from the *Swift* UVOT and XRT observations of the sample, (as well as upper limits assuming $\Gamma_X = 2$, when applicable). We compute unabsorbed X-ray flux densities at 2 keV using the PIMMS v4.10 web tool⁷. Following Eq. 4 of Tananbaum et al. (1979) and Eq. 11 of Grupe et al. (2010), the definition of this ratio is $\alpha_{\text{OX}} = 0.3838 \log(L_{2 \text{ keV}}/L_{2500\text{\AA}})$. Of the transients detected in X-rays, the α_{OX} of ZTF19abvgxrx evolves over 150 days between 1.1 and 1.4, and ZTF19aailpw1 is observed in X-rays during only one epoch with $\alpha_{\text{OX}} = 1.7$, equivalent to that of the late time detections of ZTF19aaiqmg1. The range of α_{OX} measured for the sample is consistent with that of NLSy1s ($0.9 < \alpha_{\text{OX}} < 1.8$; Gallo 2006).

3.2. Spectroscopy

From the FWHM of the broad Balmer emission lines, we classified all sources in the sample as NLSy1s. We fit the H α and H β line profiles of the host (when available) and transient spectra of the sample with the non-linear least-squares minimization and curve-fitting routine in the `lmfit` Python package. The results of these fits are shown in Figure 5. Using a Lorentzian profile for the broad H α component fit provided an improvement of the fit over that of a Gaussian profile, as would be expected based on studies of NLSy1s (e.g. Nikolajuk et al. 2009).

We compare the host (when available) and transient spectra of this sample to other transients in NLSy1s in Figures 6 (showing the full wavelength range of the observations) and 7 (rest wavelength 3700 – 5150 Å, showing clearly the He II, Fe II, and H β line profiles). In Figure 7 we color-code the sample (as well as these known NLSy1-related transients in the literature) based on the observational classification scheme we establish in Section 4.3, named after the features discussed in the fol-

lowing sections: “He II only”, “He II+N III”, and “Fe II only”⁸.

When compared to the newly discovered flaring events to those in the literature, it is clear that AT2017bgt (Trakhtenbrot et al. 2019a) has a much stronger He II+N III Bowen fluorescence profile, CSS100217 (Drake et al. 2009) has stronger narrow emission lines overall, and ZTF18aajupnt (Frederick et al. 2019) has a weaker blue continuum. The presence and strength of Fe II is uncorrelated with other spectroscopic properties of the transients shown. Of the ZTF sample, the transient spectrum of ZTF19aatubsj shows the strongest Fe II complex. However, ZTF19aatubsj shows no strong He II + Bowen fluorescence features while the others in the ZTF sample do. ZTF19aatubsj and ZTF19aaiqmg1 both show offset blue components of H β .

3.2.1. Strong He II profiles in AGN?

In the discovery paper for transient ASASSN-18jd, Neustadt et al. (2020) emphasized the relatively rare nature of strong He II emission in AGN in general, noting the exceptions in the Trakhtenbrot et al. (2019a) observational class of flares as well as the rapid changing-look AGN event ZTF18aajupnt (Frederick et al. 2019). A strong He II line profile is common (but not ubiquitous) in the spectra of TDEs, and they are typically accompanied by Bowen fluorescence features (e.g. Blagorodnova et al. 2019; van Velzen et al. 2020b). ZTF19aaiqmg1, ZTF19abvgxrx, ZTF19aailpw1 look the most similar to AT2017bgt spectroscopically. They are spectroscopically classified as “He II+N III”-type flares in Figure 7.

3.2.2. The Fe II complex

A strong Fe II line complex (blueward and redward of H β + [O III] in optical spectra, between 4434 Å and 5450 Å) is a distinguishing feature of NLSy1 galaxies. Reverberation mapping studies of AGN show that the line complex emitting region is measured farther than the Balmer line emitting region (e.g. Barth et al. 2013; Rafter et al. 2013). The Fe II complex seen in PS16dtm was interpreted as evidence of the system being a NLSy1 prior to the onset of the flare. CSS100217 also displayed a strong Fe II complex and was interpreted as a SN in a NLSy1 (Drake et al. 2011). TDE AT2018fyk also showed low ionization lines including an Fe II (37,38) emission multiplet emerging for 45 days during the tidal disruption event, and forms a class of Fe-rich TDEs along with ASASSN-15oi and PTF-09ge (Wevers et al. 2019). Therefore, this feature may indicate the presence of an AGN, but is not always useful in determining the nature of a particular AGN-related flare. For two of the transients in this sample, whether or not the Fe II

⁶ We note that ASASSN-15lh showed a large amplitude “double-humped” structure in its UV light curve.

⁷ <https://cxc.harvard.edu/toolkit/pimms.jsp>

⁸ We note that although “only” is used in the categorization naming based on the presence of spectral features, all have strong Balmer features.

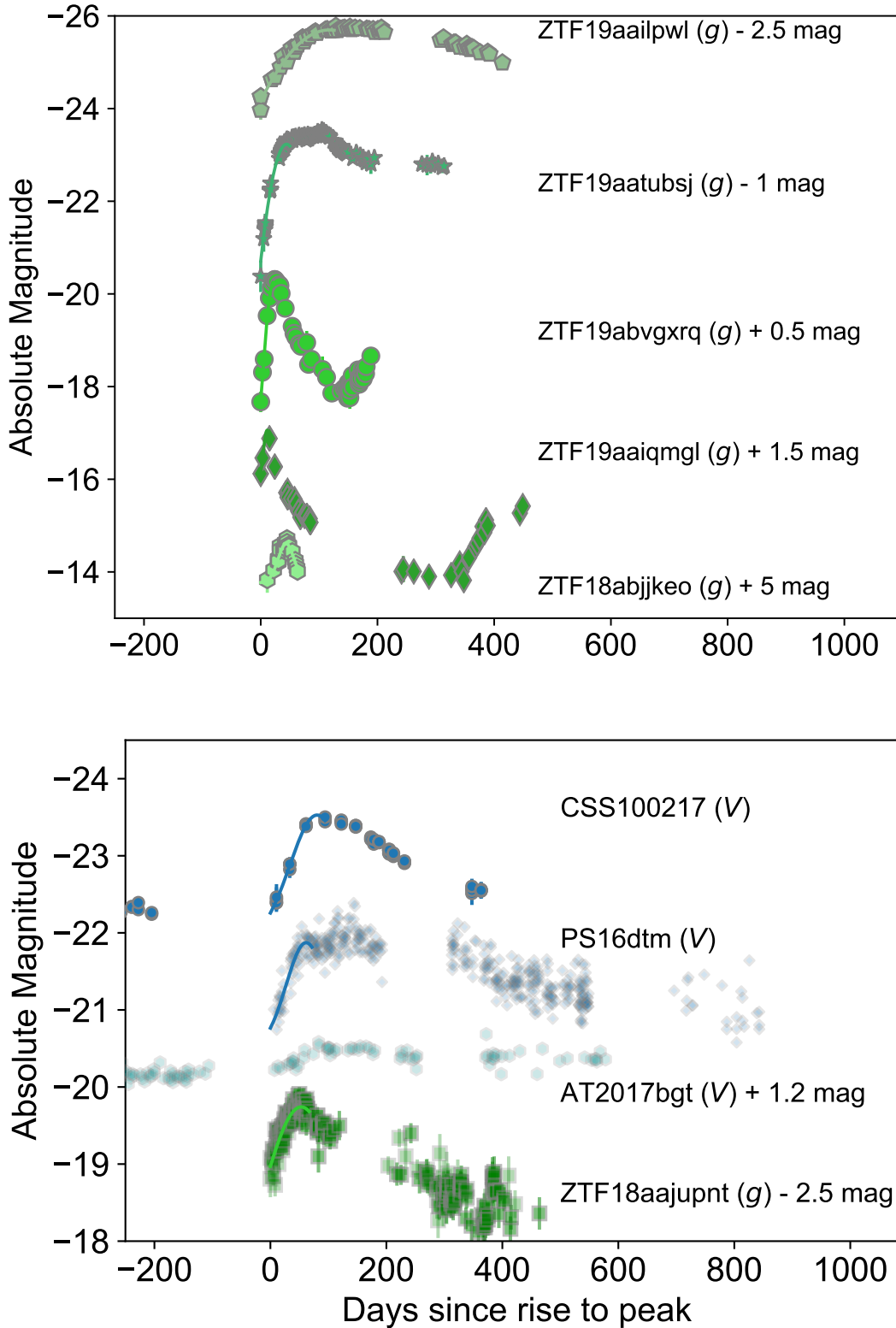


Figure 3. The difference imaging light curves of the ZTF sample (upper panel) compared to the published light curves of NLSy1-related events from the literature (lower panel): changing-look LINER ZTF18aajupnt (Frederick et al. 2019), TDE in a NLSy1 PS16dtm (Blanchard et al. 2017), SN in a NLSy1 CSS100217 (Drake et al. 2011), and the aperture photometry of flaring NLSy1 AT2017bgt (Trakhtenbrot et al. 2019a). We show only *g*-band observations for the ZTF sample (upper panel), and omit errorbars for visual purposes. Note the differences in optical filters shown (*g* in green, *V* in blue), the differences in colors and markers used to represent the same filters for visual clarity, as well as the difference in y-axis scale between the panels. CRTS data for CSS100217 > 200 days prior to the transient is not shown on this scale, but showed no significant activity for > 5 years.

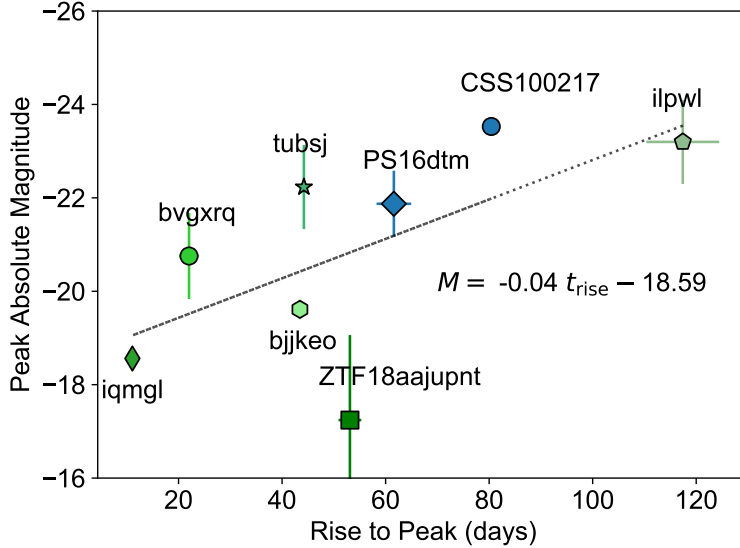


Figure 4. Correlation of the rise times of the sample light curves with the maximum absolute magnitude. Fits to light curves are described in Section 3.1.1. The same color scheme and markers are used as in Figure 3.

complex can be seen in optical spectra depends on the phase and the continuum brightness of the transient — for ZTF19aatubsj it was not observed for 368 days, and for ZTF19aaiqmgl it became no longer visible during the second rise 444 days after the initial spectrum was taken.

3.3. X-rays

There are only two significantly X-ray detected transients in the sample: ZTF19abvgxrq and ZTF19aaiqmgl. We show their X-ray spectra in Figure 8 fit to power law models. The third, ZTF19aailpwl, was only detected in one epoch and not at a level that allowed for the signal-to-noise necessary for a spectrum.

The X-ray spectrum of ZTF19abvgxrq is measured by *Swift XRT* with a power law index of $\Gamma = 2.99 \pm 0.02$, typical of the strong soft X-ray excess observed below 1 keV in NLSy1s ($\bar{\Gamma} = 2.8 \pm 0.9$; Boller et al. 1996; Forster & Halpern 1996; Molthagen et al. 1998; Rakshit et al. 2017). The spectrum of ZTF19abvgxrq could also be explained by a 150 eV blackbody with a $\Gamma = 2$ power law component and no intrinsic absorption (Kara et al. 2019). We note that the soft excess observed in NLSy1s can mimic the blackbody temperatures expected for TDEs (e.g. Boller et al. 1996).

The spectral index of ZTF19abvgxrq ($\Gamma \sim 3$) was similar to that of AT2018fyk, interpreted as a TDE with late-time disk formation (Wevers et al. 2019), as well as ZTF18aajupnt, interpreted as a changing-look LINER “turning-on” into a NLSy1 (Frederick et al. 2019). The X-ray spectral index of ZTF19aaiqmgl was quite high even with regard to these events, with $\Gamma \sim 4 - 6$.

3.4. Black Hole Masses

We measured the black hole masses of the sample using two different methods, each with important caveats: The virial mass method, which may systematically underestimate BH masses for NLSy1s, and the host galaxy luminosity, which may be contaminated by the presence of an AGN. The M_{BH} calculated from the host galaxy luminosity is $M_{\text{BH},M_r} = -0.5M_{r,\text{host}} - 2.96$ following McLure & Dunlop (2002), and the standard virial method (e.g. Shen et al. 2011) was employed to obtain the virial black hole masses from FWHM $H\beta$ reported in Table 2. The transient Eddington ratio estimates depend on the BH masses (M_{BH}) as $L_{\text{Edd}} = 1.3 \times 10^{38} (M_{\text{BH}}/M_{\odot}) \text{ erg s}^{-1}$. For each transient in the sample, we report a range of Eddington ratios in Table 2 bracketed by the Eddington ratio measured assuming the virial mass estimate for the BH mass, and the Eddington ratio measured assuming BH mass derived from the host galaxy luminosity. The range in BH masses, and therefore Eddington ratios, shown in Table 2 is quite large. We estimate statistical and systematic uncertainties of 0.3–0.5 dex on these mass and Eddington ratio measurements, due to the typical scatter associated with single-epoch mass scaling relationships as well as the unknown BLR geometry (e.g. Merloni et al. 2015; Runnoe et al. 2016; Liu et al. 2018a, 2020).

Miller et al. (2019) obtained an independent measurement of the BH mass of ZTF19abvgxrq. They measured $M_{\text{BH}} = 3.7 \times 10^6 M_{\odot}$ from the observed Chandra X-ray luminosity (this observation is described in more detail in Section 2.4). This is closer to, but not consistent with, the virial mass estimate, meaning that the transient may not have been accreting near the Eddington limit at the time of the X-ray observation.

Table 2. Black hole mass measurements of the sample from optical spectra and host galaxy properties. NLSy1s are typically thought to be lower mass, highly accreting systems, but we show here that the uncertainty in the mass estimates generates significant uncertainty in the estimates of the Eddington ratios (described in Section 3.4). $M_{r,\text{host}}$ is the r -band de Vaucouleurs and exponential disk profile model fit magnitude from the SDSS DR14 photometric catalog. The host of ZTF18abjjkeo is not in the SDSS footprint, and so we instead use the Pan-STARRS1 r -band Kron magnitude of this source (Chambers et al. 2016).

Name	$M_{r,\text{host}}$	$\lambda L_{5100\text{\AA}}$	$\text{FWHM}_{H\beta}$	$\log M_{\text{BH},M_r}$	$\log M_{\text{BH},\text{vir}}$	L/L_{Edd}
	(mag)	(10^{43} erg s $^{-1}$)	(km s $^{-1}$)	[M_{\odot}]	[M_{\odot}]	
ZTF19abvgxrxq	-21.36	5.00 ± 0.04	878 ± 49	7.7	6.4	0.066-1.5
ZTF18abjjkeo	-20.94	2.24 ± 0.02	1199 ± 270	7.5	6.4	0.048-0.62
ZTF19aailpwl	-22.38	42.6 ± 0.8	$1050 \pm 77^{\text{a}}$	8.2	7.2	0.17-1.97
ZTF19aaiqmgl	-20.35	0.553 ± 0.008	1433 ± 35	7.2	6.1	0.023-0.29
ZTF19aatubsj	-21.51	21.9 ± 0.2	1208 ± 57	7.8	7.1	0.24-1.2

a. The $\text{FWHM}(H\beta)$ for ZTF19aailpwl agrees with the measurement in Rakshit et al. (2017) within the error estimates.

4. DISCUSSION

In this section, we rule out possible physical scenarios for each outburst, beginning with core collapse supernovae II n . We review why the supernova interpretation was quickly ruled out in favor of a supermassive black hole accretion scenario, and discuss how many of the characteristics of the objects are consistent with both NLSy1s and TDEs. We compare the available evidence with other scenarios including TDEs, extreme AGN variability, and binary SMBHs in detail. We also discuss NLSy1 galaxies as the preferential hosts for these and other similar events, and outline a scheme for classifying future events based on the presence of spectral features.

4.1. “II n or not II n ?”: Preliminary Observational Classification of the Flare Sample

Identification of the sample presented here occurred with a slew of conflicting preliminary classifications at early times, which we describe below.

The narrow emission lines in the spectra of some SLSN (Type II n) are a result of the highly luminous interaction of supernova ejecta from a massive progenitor with dense circumstellar medium. Therefore, under special circumstances, nuclear SNe can look spectroscopically very similar to rapid⁹ flares from NLSy1s in the optical (e.g. Moriya et al. 2018). The shapes of the light curves of the transients in this sample looked rather like those of such supernovae, in the absence of additional observations. The smoothness of the flares in particular was unique with respect to typical stochastic AGN variability, and made these transients noteworthy for allocation of follow-up resources. Therefore, the narrow Balmer features in the spectra of these transients, coupled with their light curve shapes, left uncertainty in their early

classifications. They could have been either Type II n supernovae or NLSy1 AGN, while those with persistent strong He II $\lambda 4686$ features in their spectra looked similar to that of TDEs. To illustrate this, Figure 9 shows spectra of the sample alongside a Type II n SN as well as a TDE with Bowen fluorescence features. Additional follow-up observations in the UV/X-rays helped distinguish this sample of transients from SNe.

4.2. A Preponderance of Rapid Optical Transients in Narrow-line Seyfert 1 Host Galaxies

In the Analysis section (§3), we compared our sample to data from nuclear transients in the literature that happened to be hosted in NLSy1 galaxies. In this and the next sections, we discuss NLSy1s as an interesting AGN subtype, and observationally classify and link these events to one another on the basis of their shared host properties.

The narrower broad-line Balmer profiles and high amplitude variability, (especially in the X-rays, e.g. Pogge 2000; Frederick et al. 2018) in NLSy1s may be evidence of smaller black hole masses in these systems ($5 < \log(M_{\text{BH}}[M_{\odot}]) < 8$; e.g. Mathur et al. 2001), and/or higher observed accretion rates (Pounds et al. 1995; Wang et al. 1996; Marconi et al. 2008; Grupe et al. 2010; Xu et al. 2012). The virial masses derived from spectral measurements of the population may also be explained with geometrical effects, when interpreted as the classic broad-line AGN seen along a lower inclination angle between the broad-line emitting region and the line of sight (Decarli et al. 2008; Baldi et al. 2016; Rakshit et al. 2017).

Studies of NLSy1s typically find them to be highly photometrically variable only in the X-rays. At optical wavelengths, however, Klimek et al. (2004) found that rapid, high amplitude variability was rare in a sample of 172 observations of NLSy1s across 33 nights. Ai et al. (2010) also found that NLSy1s had systematically lower optical variability amplitudes ($\lesssim 0.2$ mag) than broad-

⁹ With rise times on the order of days to weeks.

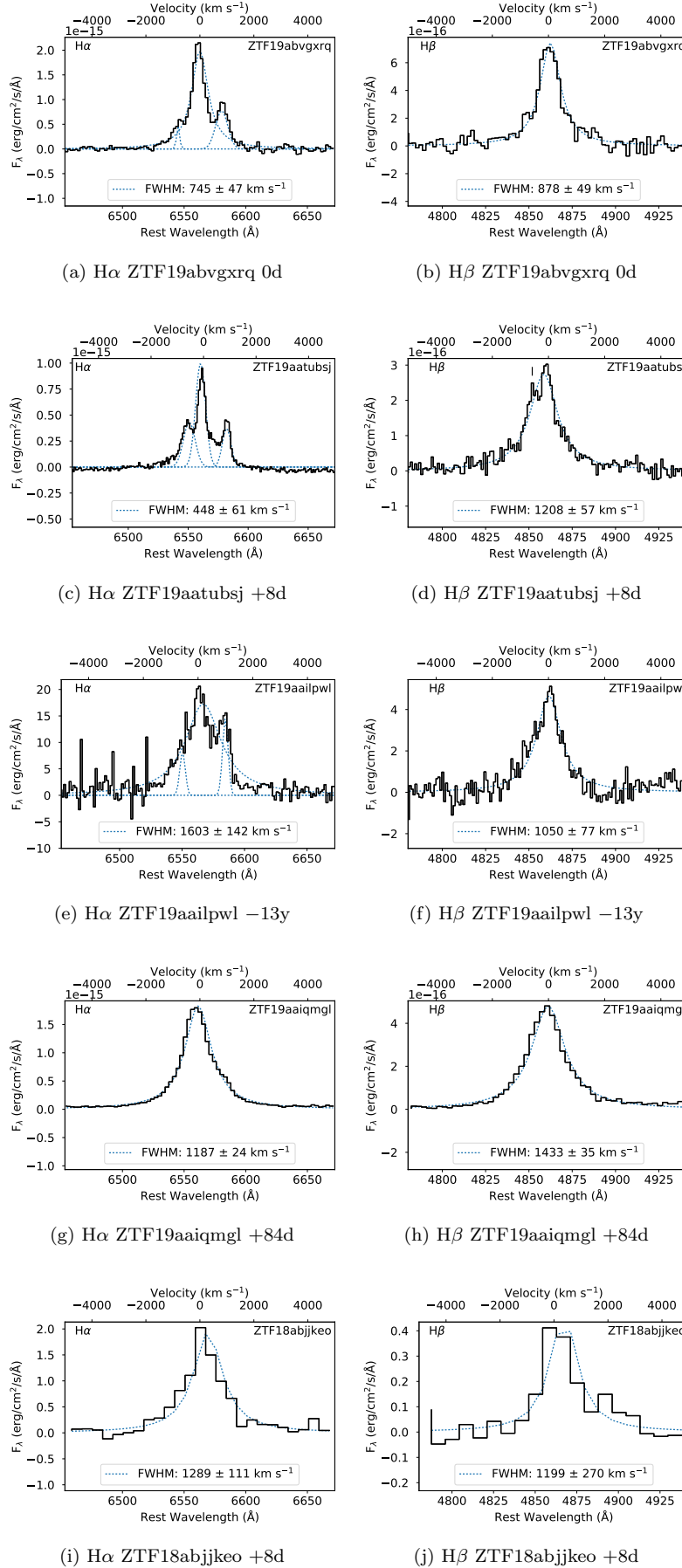


Figure 5. Gaussian fits to the $H\alpha$ + $[N\ II]$ and $H\beta$ line profiles of all transients in the sample show that their Balmer lines have a FWHM consistent with (and Lorentzian Balmer profiles characteristic of) that of narrow-line Seyfert 1s. The offset blue peak in the $H\beta$ profile of ZTF19aatubsj is marked by a vertical line.

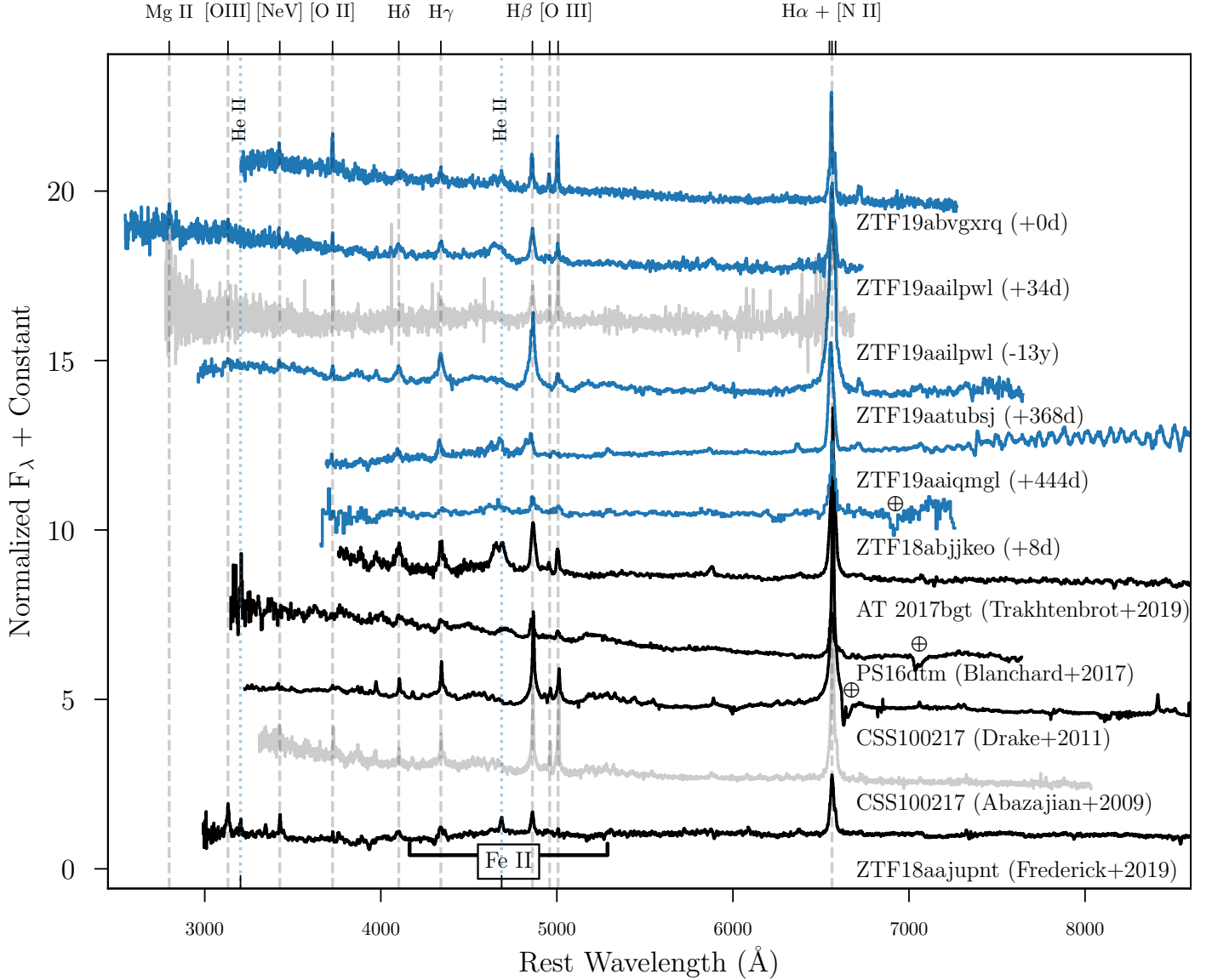


Figure 6. Comparison of the ZTF sample of flares (in blue), as well as discovery spectra for the NLSy1-related events from the literature (in black): changing-look LINER ZTF18aajupnt (Frederick et al. 2019), TDE in a NLSy1 PS16dtm (Blanchard et al. 2017), SN in a NLSy1 CSS100217 (Drake et al. 2011), and Bowen fluorescent flare AT2017bgt (Trakhtenbrot et al. 2019a), and their pre-event spectra when available (in grey). For ZTF19aatubsj and ZTF19aaiqmgl here and in Figure 7, we plot the spectra after continuum fading rather than the discovery spectra, to display the features used in the spectroscopic classification scheme discussed in Section 4.3. ZTF19aatubsj and ZTF19aaiqmgl show offset blue peaks in H β , and the peak of He II is offset from 4686 Å in ZTF18abjjkeo.

line Seyfert 1s in a sample of 275 AGN at $0.3 < z < 0.8$ in 3 years of SDSS data.

However, optical flares are not unheard of in NLSy1s (e.g. NGC 4051, Guainazzi et al. 1998; Uttley et al. 1999). Klimek et al. (2004) noted the exception of IRAS 13224-3809, which showed both dramatic X-ray and optical variability on short timescales (Miller et al. 2000). Here we describe a number of distinct events, including

the Trakhtenbrot et al. (2019a) observational class of optical flares, the “on” state of ZTF18aajupnt, and the host of PS16dtm and CSS100217:102913+404220, which were all consistent with NLSy1 related activity.

Trakhtenbrot et al. (2019a) established a new observational class of dramatic AGN flares accompanied by Bowen fluorescence features. The events in this class all originated from active black holes that were classified as

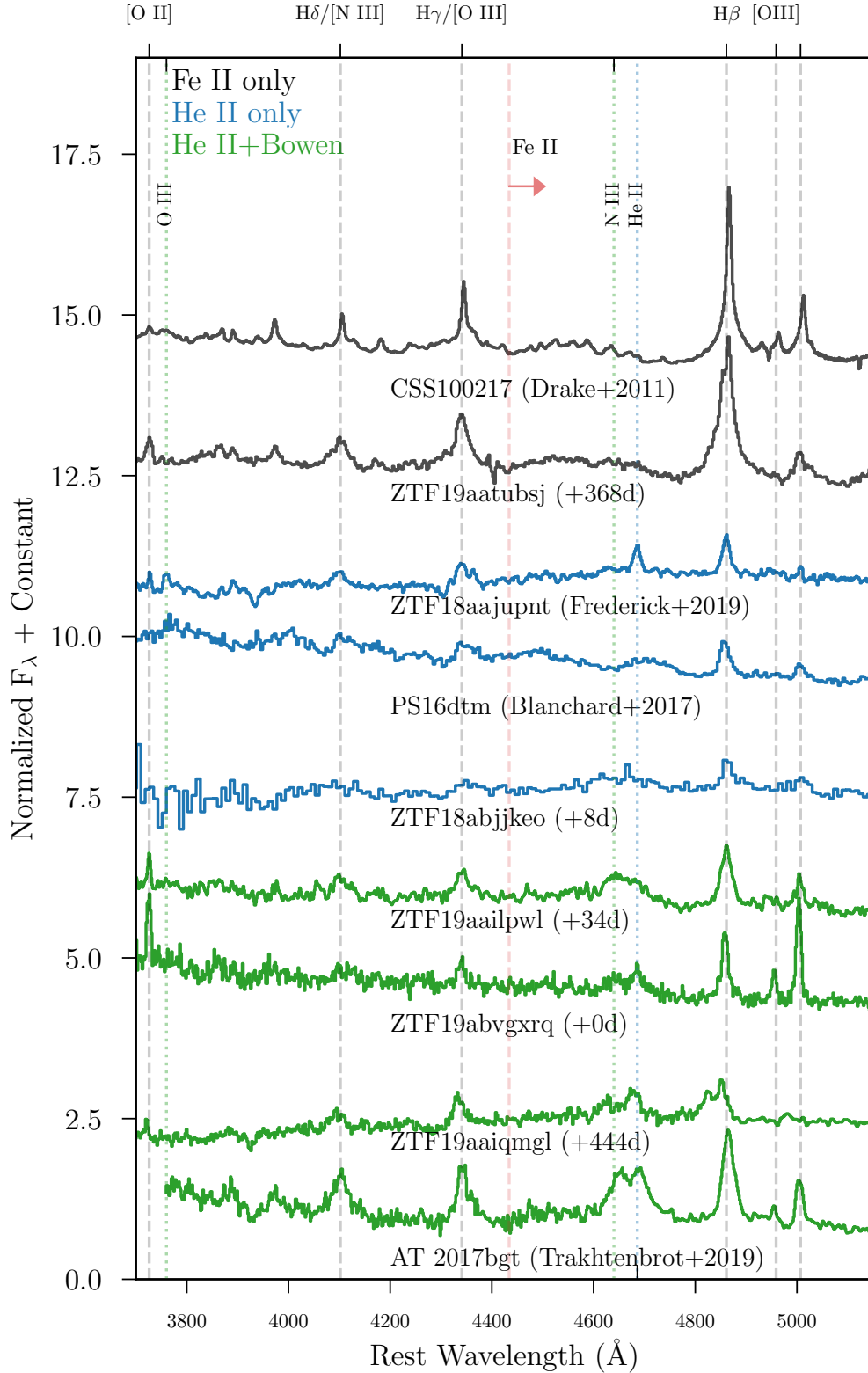


Figure 7. Zoom-in on the 4000-5000 Å region of Figure 6 showing the comparison of the strength of H β , Fe II, and [O III] of the sample with NLSy1-related events in the literature. We color-code the sample and establish categories based on the presence and absence of key emission line features as described in Section 4.3. Blue spectra indicate the presence of He II, and black spectra indicate transients which displayed Fe II only, (though we note that PS16dtm showed both features). Those in green display Bowen fluorescence features in addition to He II, and are most spectroscopically similar to AT2017bgt and the other AGN flares comprising the sample in Trakhtenbrot et al. (2019a).

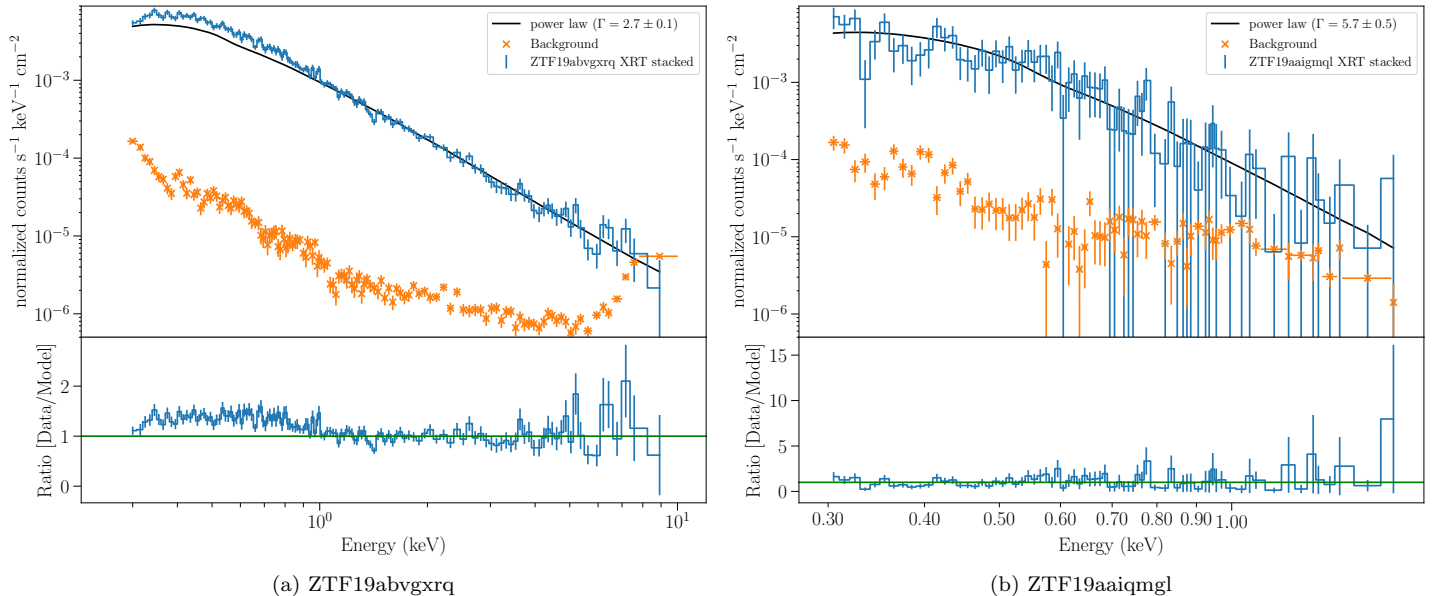


Figure 8. Left panel: An absorbed power law fit and ratio residuals to the ~ 100 ks stacked *Swift XRT* spectrum of ZTF19abvgxrq (spectral index $\Gamma = 2.7 \pm 0.1$). Right panel: The ~ 4 ks stacked spectrum of ZTF19aaiqmg1 ($\Gamma = 5.7 \pm 0.5$).

NLSy1 galaxies by their Balmer FWHMs. Their optical spectra were unusual for NLSy1s in that they showed strong “double-peaked” He II profiles with contributions from the N III $\lambda 4640$ Bowen fluorescence feature, indicating the presence of a strong UV ionizing continuum. This was consistent with the UV brightness observed in the small sample of objects as well as the steep blue continua in these sources. The slow UV and spectral emission line evolution over a period of ~ 450 days ruled out a TDE, and these were instead interpreted as enhanced accretion onto the SMBH of a pre-existing AGN. AT2017bgt was presented as the prototype of these dramatic SMBH UV/optical flares irradiating the BLR. It showed a very slow decrease in optical flux over several months following a relatively shallow (~ 0.5 mag) rise to peak over ~ 80 days from a previous non-variable state. During the transient, the X-rays increased by a factor of 2–3 from a previous measurement by ROSAT. The persistence of the UV emission over 500 days distinguished it from SNe, and the extremely intense nature of the UV continuum as well as presence of the Bowen fluorescence features in the optical spectrum distinguished it from CLAGN. Two other NLSy1s, OGLE17aaj (Gromadzki et al. 2019) and ULIRG F01004-2237 (Tadhunter et al. 2017) (the latter previously interpreted as a TDE), were retroactively reclassified as belonging to this new observational class of NLSy1s.

We compare with ZTF18aajupnt, a changing-look AGN which transformed from a LINER galaxy to a NLSy1. It was identified as such primarily based on X-ray and UV spectra. It displayed strong high ionization forbidden (i.e. “coronal”) emission in the optical and UV spectra, an X-ray flare delayed by 60 days,

and showed a late-time $g - r$ color change as it faded slowly over 1 year. This was the only AGN with Balmer lines consistent with a NLSy1 among a new class of “changing-look LINERs”, including SDSS 1115+0544 (Yan et al. 2019).

PS16dtm (iPTF16ezh/SN 2016ezh) was a near-Eddington but X-ray-quiet nuclear transient with strong Fe II emission and $T_{\text{BB}} \sim 1.7 \times 10^4$ K. It rose over ~ 50 days to “superluminous” levels ($\log L_{\text{bol}} [\text{ergs s}^{-1}] > 44$) at peak before plateauing twice over ~ 50 and ~ 100 days while maintaining a constant blackbody temperature. The event was interpreted as a TDE exciting the BLR in a well studied, spectroscopically-confirmed NLSy1 with $M_{\text{BH}} \sim 10^6 M_{\odot}$ (Blanchard et al. 2017). X-ray upper limits showed dimming by at least an order of magnitude compared to archival observations, but Blanchard et al. 2017 predicted the X-rays would reappear after the obscuring debris (oriented perpendicularly to the accretion disk) had dissipated. We show the V -band ASASSN photometry for PS16dtm in Figure 4 which appears similar in shape and absolute magnitude to ZTF19aatubsj, though longer in duration.

CSS100217:102913+404220 displayed a high state ($M_V = -22.7$ at 45 days post-peak) accompanied by broad H α and was interpreted either as a Type IIIn SN (Drake et al. 2011) or a TDE (Saxton et al. 2018) near the nucleus (~ 150 pc) of a NLSy1 in a star forming galaxy. It eventually faded back to slightly below its original level after one year, which was interpreted as interacting with and subsequently flushing a portion of the accretion disk.

Similar events are not unheard of in broad-line AGN systems, though they may be comparatively more rare.

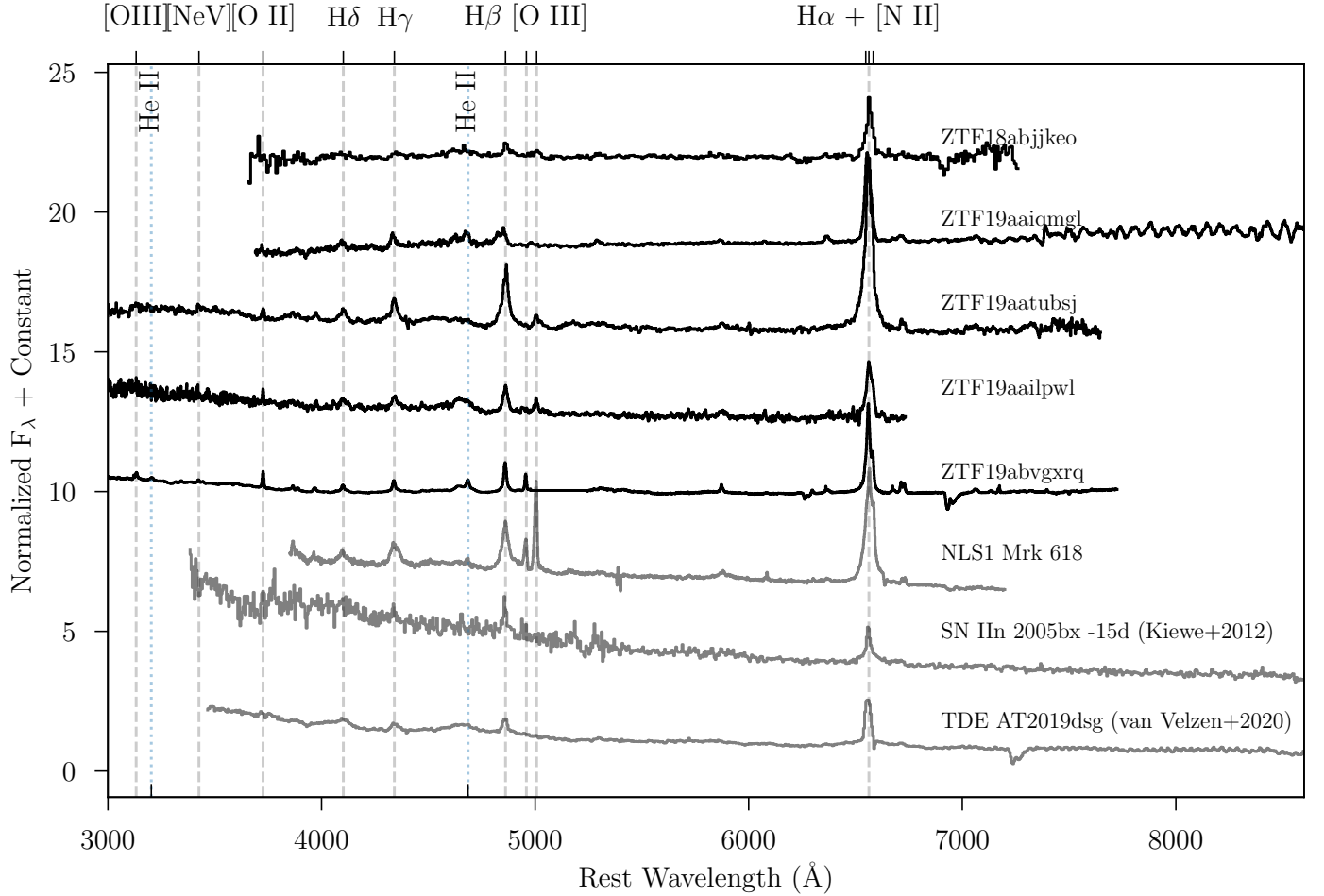


Figure 9. We compare the spectra of the transient sample (in black) to archetypal NLSy1 Mrk 618, as well as a normal Type IIIn supernova, SN 2005bx (Kiewe et al. 2012), and AT2019dsg, a normal TDE in a star forming galaxy with Bowen fluorescence features and a coincident neutrino detection (van Velzen et al. 2020b; Stein et al. 2020).

Neustadt et al. (2020) reported a candidate for such a rapidly flaring event with quasar-like properties, ASASSN 18jd, although continued observations of this transient will be critical for a better understanding of the properties of the host.

4.3. Observational Classification: The “Family Tree” of NLSy1-associated Transients

In Table 3, we use this sample to motivate a framework for quickly classifying similarly ambiguous flaring events. We investigate the following:

- AGN/NLSy1 characteristics (an empirical $W1 - W2$ WISE color cutoff from Stern et al. 2012; Assef et al. 2013, which is comparable between NLSy1s and broad-line Seyfert 1s; Chen et al. 2017; a strong Fe II complex; narrow Balmer emission; and $[O III]/H\beta < 3$; Rakshit et al. 2017),

- TDE characteristics (host black hole mass below the Hills mass ($\sim 10^8 M_\odot$), and a lack of cooling or significant rebrightening),
- X-ray properties (the presence of which can occur in both AGN and TDEs, but are less likely in the SN scenario).

We apply these criteria in Table 3 and color code them as blue or green based on whether they favor the TDE or AGN scenario, respectively (as the SN scenario has been ruled out in Section 4.1). The spectroscopic class, based on the presence of N III Bowen fluorescence features, Fe II, and/or He II $\lambda 4686$, which can occur in both TDEs as well as flaring NLSy1s, is then interpreted in the context of one of these scenarios. Based on this table, we confirm the interpretations for three of the four NLSy1-associated transients reported in the literature, except for CSS100217 for which we favor the AGN scenario over the SN interpretation.

Summarized briefly: We expect transients with strong Fe II complexes are most likely associated with AGN, those with very steep soft X-ray spectra ($\Gamma > 5$) and no intrinsic absorption are most likely associated with TDEs, and those with strong Bowen fluorescence profiles and slow UV and spectral evolution are likely associated with enhanced accretion onto supermassive black holes from a pre-existing accretion disk. The timing of a mid infrared flare may also help to distinguish between an AGN and a TDE — if it precedes the optical, it is likely associated with AGN variability, but if it follows as an echo, it may be associated with a TDE (van Velzen et al. 2016).

van Velzen et al. (2020b) established a spectroscopic classification scheme for the sample of TDEs discovered during the first half of the ZTF survey, distinguishing those with and without He II in a single epoch. About half of the TDEs in that sample were “H-only”, and only one was “He-only”. They found that higher density conditions were likely for the rest of the TDEs which had H and He lines, as well as Bowen features.

For the flaring NLSy1 sample presented here, we establish the following spectroscopic classes to describe each of the transients based on the presence or absence emission features crucial to their physical interpretations:

1. “He II only”,
2. “He II+N III”, and
3. “Fe II only”,

and we propose the following naming convention for these classes: “NLSy1-HeII”, “NLSy1-HeII+NIII”, and “NLSy1-FeII”.¹⁰

4.4. Physical Interpretation of the Transient Flares

In the following section we consolidate all that is known about the relevant properties of each object in the sample, and compare them with the related transients in NLSy1s in the literature, to explore each of the following scenarios: A PS16dtm-like TDE in a NLSy1, A Sharov-21-like microlensing event, a CSS100217-like SN in a NLSy1, and a binary SMBH scenario.

4.4.1. Association of the Transients with AGN

There is evidence that all sources in the sample are associated with AGN rather than distinct explosive events occurring in a normal galaxy. Although these outbursts may not necessarily be the result of an intrinsic enhancement in AGN accretion activity, transients with fast-rise/slow-decay (such as those in this sample, along with

slow-rise/fast-decay, and symmetric light curve shapes) were well-represented in a sample of 51 AGN flares discovered in CRTS (Graham et al. 2017).

Rakshit et al. (2017) spectroscopically classified the SDSS spectrum of the host galaxy of ZTF19aailpwl as harboring an AGN NLSy1 > 12 years prior to the onset of the smoothly flaring transient reported here.

As evident in Figure 9, the strengths of the Balmer lines in the transient spectra are most consistent with that of a NLSy1. Ne V $\lambda 3426$, when observable, is typically associated with AGN, and is present in the spectra of these sources. Strong He II profiles, although somewhat rare in association with normal stochastic AGN variability (Neustadt et al. 2020), have been observed before and interpreted as the signature of a sudden enhancement of accretion (e.g. Trakhtenbrot et al. 2019a; Frederick et al. 2019).

Persistent X-rays are a likely signature of accretion onto a SMBH rather than a SN. A strong soft X-ray excess is characteristic of NLSy1s. However, it is typically accompanied by a hard X-ray continuum component (not present in either X-ray detected transient in this sample), and not nearly as ultra-soft as the X-rays seen in ZTF19aaiqmgl ($4 \lesssim \Gamma \lesssim 6$), which are slopes more frequently observed in the X-ray spectra of TDEs.

4.4.2. The SN Scenario

It is highly improbable that these flares are the result of normal SN explosions. We observe long-lived *U*-band emission in ZTF19aatubsj, persistent UV emission in all transients in the sample, and strong transient X-ray detections in ZTF19abvgxrq and ZTF19aaiqmgl. There is also only a small likelihood of a SN in the host galaxy along the line of sight unassociated with the AGN. The strongest evidence against the normal supernova scenario is the persistence of the He II emission features $\sim 10 - 100$ days after the onset of the flare — such flash ionization signatures are only visible in supernova spectra at very early times (e.g. Khazov et al. 2016; Bruch et al. 2020).

At least one of these transients (ZTF19aatubsj) shares a number of properties with CSS100217, which displayed soft X-rays and was interpreted as a SN IIn explosion in an AGN disk. The SN interpretation of CSS100217 was largely based on light curve energetics, which are similar to those of this sample. The $g - r$ color change, and the peak magnitude of $-23 \lesssim M_V \lesssim -22$ are very similar in particular between CSS100217 and ZTF19aatubsj. Type IIn supernovae can exhibit strong Fe II lines in late spectra, such as ZTF19aatubsj did.

However, in contrast, the light curve evolution differs in that CSS100217 fades at least twice as quickly as ZTF19aatubsj. Also, the Fe II complex of CSS100217 was always visible throughout the flare, and Drake et al. (2011) observed a broad ~ 3000 km s⁻¹ component in H α which got broader with time in subsequent follow-up spectra of CSS100217. Strong P Cygni profiles

¹⁰ We note that although hydrogen features are not explicitly named in this feature classification scheme, all spectra of the transients show resolved narrow ($1000 < \text{FWHM} < 2000$ km s⁻¹) Balmer features (see Section 3.2).

Table 3. Comparison of the properties of individual objects in the sample (upper table) and NLSy1-related transients in the literature (lower table). "✓" means that property is observed, and "×" indicates that characteristic was not observed. "UV-bright" refers to the persistence of UV-brightness, and "Rebrighten" refers to a significant recovery of at least half the peak luminosity of the source. Following the convention of Figure 7, blue (green) indicates a property associated with the TDE (flaring AGN) scenario.

Name	$\log M_{\text{BH}} < 8$ [M_{\odot}]	$H\beta < 2000$ km s $^{-1}$	Fe II	[OIII]/ $H\beta < 3$ [flux ratio]	$\Delta g - r$ ~ 0 mag	UV-bright	X-ray Γ	W1-W2 > 0.7 mag ^a	Re- brighten	Spec. class	Interp.
ZTF19abvgxrx	✓	✓	×	✓	✓	✓	3	×	✓	HeII+NIII	AGN
ZTF19aailpwl	×	✓	✓	✓	✓	✓	✓ ^b	✓	×	HeII+NIII	AGN
ZTF19aatubsj	✓	✓	✓	✓	×	✓	×	×	×	FeII	TDE
ZTF19aaiqmgl	✓	✓	✓	✓	×	✓	5	×	✓	HeII+NIII	AGN
ZTF18abjjkeo	✓	✓	×	✓	✓	-	-	×	×	HeII	TDE
CSS100217	✓	✓	✓	✓	×	✓	3	✓	×	FeII	AGN
PS16dtm	✓	✓	✓	✓	✓	✓	2 ^c	×	×	HeII+FeII	TDE
AT2017bgt	✓	✓	✓	✓	✓	✓	2	×	✓	HeII+NIII	AGN
ZTF18aaajupnt	✓	✓	×	✓	×	✓	3	×	×	HeII	AGN

a. We select the less conservative color cut presented in Stern et al. (2012).

b. The single low level *XRT* detection of ZTF19aailpwl occurred only once throughout the follow-up campaign and was not enough to take a reliable spectral measurement.

c. The host of PS16dtm displayed X-rays only prior to and following the fading of, but not for the duration of, the transient.

are observed in the optical spectra of SN, and from such profiles we would expect an absence of absorption on the blue end of the Balmer line profiles, rather than emission as in the spectra of ZTF19aaiqmgl and ZTF19aatubsj. Therefore, based on this evidence we rule out the SN Type IIn scenario.

4.4.3. The TDE Scenario

The Hills mass is the mass for which the tidal Roche radius is equivalent to the gravitational Schwarzschild radius of the black hole, beyond which a star (that would otherwise be tidally pulled apart) is instead left intact as it passes the event horizon (Hills 1975). This maximum mass to tidally disrupt a solar-type star just outside the event horizon is $10^8 M_{\odot}$. Therefore a SMBH mass significantly above this limit would likely rule out a TDE. Of the supermassive black hole masses derived for the host galaxies, only that of ZTF19aailpwl is inconsistent with a TDE scenario, (although we note that it is consistent within the typical uncertainty for such mass measurements). The range of absolute magnitudes of the flares in this sample ($-23 < M_r < -19$ mag) also tend to be intrinsically brighter at peak than all but one of the ZTF TDEs ($M_r > -20$ mag) reported in van Velzen et al. (2020a), AT2018iih ($M_r = -21.5$ mag).

Similar to TDEs PS16dtm and AT2018fyk, ZTF19aatubsj showed two distinct plateau stages on month-long timescales after fading, with some slight fading in between. Color evolution is rare but not unheard of for TDEs, and the cooling ZTF19aatubsj shows post-peak is slow, with the transient still detected in

the UV at late times as would be expected for a TDE. Optical rebrightening following the initial flare has been interpreted as the result of late time disk formation in a number of TDEs (e.g. Wevers et al. 2019; van Velzen et al. 2019). However, rebrightening with high amplitudes returning nearly to pre-flare levels such as that seen in ZTF19abvgxrx and ZTF19aaiqmgl has neither been observed¹¹ nor predicted (e.g. Chan et al. 2019, 2020) from a TDE. In these cases with rebrightening, a TDE is strongly ruled out.

ZTF19aaiqmgl and ZTF19aatubsj, like AT2018fyk, only showed Fe II at certain times during the flare. ZTF19aaiqmgl only displayed Fe II during its first peak, and in ZTF19aatubsj, the Fe II complex got more visible as the transient faded. ZTF19aatubsj is the only transient in the sample with a lack of He II features in its spectra. Within the van Velzen et al. (2020b) spectral classification scheme for optical TDEs, ZTF19aatubsj would be a H-only TDE, with the Fe II complex attributed to the NLSy1 host. It is important to note that the transients with blue horn features in $H\beta$, ZTF19aaiqmgl and ZTF19aatubsj, may be signatures of wind ejecta with a velocity distinct from the AGN.

Enhanced N III lines such as that seen in the NLSy1-HeII+NIII spectroscopic class (ZTF19abvgxrx,

¹¹ Except in the case of the periodicity of ASASSN 14ko, which was interpreted as a possible repeating partial TDE (Payne et al. 2020).

ZTF19aailpwl, and ZTF19aaiqmgl) are a prediction of TDEs in AGN when compared to the host spectrum (Kochanek 2016; Liu et al. 2018b; Gallegos-Garcia et al. 2018). Unfortunately, a pre-flare spectrum was only available to test this for ZTF19aailpwl (Figure 6).

Many properties of the hosts do not align with what we expect from AGN. The WISE colors, for example, span a broad range of 0.06–0.98 mag (Table 3). The IR flare associated with ZTF19aaiqmgl could be interpreted as a dust echo, similar to those seen in a number of TDEs (van Velzen et al. 2016). A host-subtracted SED fit to the *Swift* photometry of ZTF19aaiqmgl gives a blackbody temperature consistent with that of known TDEs, $10^{4.25}$ K.

The X-ray variability of TDEs can vary erratically during a flare (e.g. Wevers et al. 2019; van Velzen et al. 2020b). Although soft X-ray excesses with $\Gamma \sim 3$ are characteristic of NLSy1s, ZTF19aaiqmgl displays an X-ray power law index much higher than typically seen in NLSy1s, and more characteristic of the extremely soft X-ray spectra observed in TDEs.

Based on the combination of properties shown in Table 3, we conclude that two of the flares, ZTF18abjjkeo and ZTF19aatubsj, are better explained as TDEs than AGN flares, although the interpretation is not clear-cut. However, if we assume that their spectra are a combination of the host NLSy1 galaxy and the transient line emission from the TDE, then given their spectral classes given here of NLSy1-FeII and NLSy1-HeII, respectively, then the TDE spectra themselves, in these NLSy1 galaxies, would have to be of the TDE subclasses of TDE-H (H only lines) and TDE-He (He II only lines), respectively, in order to match the observed spectra.

4.4.4. The Extreme AGN Variability Scenario

Graham et al. (2017) presented a sample of quasars displaying extreme variability in CRTS. Some had similar profiles and amplitudes (rising by 2–2.5 mag) but longer timescales (500–1000 days) compared to the flares presented here. For example, J002748-055559 rose by nearly ~ 2 mag compared to the steady level it maintained for several years prior.

The optical spectra of the transients in the sample presented here belonging to the “NLSy1-HeII+NIIB” spectroscopic class, as well as the UV brightness of the sample, are consistent with the properties of the observational class of flares with Bowen fluorescence established in Trakhtenbrot et al. (2019b). However, all of the transients presented here have faster fading timescales than AT2017bgt. Trakhtenbrot et al. (2019b) stated that the fade timescale of AT2017bgt was longer than expected for a TDE. However, we note that at least one TDE in the van Velzen et al. (2020b) sample (that also displayed Bowen fluorescence features) was observed to fade over nearly 15 months,

4.4.5. The Gravitational Microlensing Scenario

Flares due to microlensing are expected to be observable in difference imaging surveys with the combined baseline of iPTF and ZTF. The rise portions of the light curve shapes of all the transients measured in Section 3.1.1 being well-fit by quadratics is consistent with a lensing event, however, all but ZTF18abjjkeo have a longer decay with respect to the initial rise. Microlensing by multiple foreground sources can give rise to a symmetric (with respect to the fade) double peak with a dip in the middle of the optical light curve such as that seen in ZTF19abvgxqr (Hawkins 1998, 2004; Schmidt & Wambsganss 2010). The cuspy shape of the first peak is also characteristic of microlensing light curves. ZTF19aaiqmgl also showed a second peak in its light curve, but the first peak was a lot more rapid and luminous than the second. To test this scenario in ZTF18abjjkeo would require continuing to observe for an additional flare.

The microlensing scenario, however, would not account for the strong transient Bowen fluorescence features that appear only at late times in ZTF19aaiqmgl, and only at early times in ZTF19abvgxqr (Figure 11). Meusinger et al. (2010) explained a similar event as a background quasar with a UV flare in J004457+4123, also known as Sharov 21, being microlensed by a foreground star in M31.

Microlensing is characteristically achromatic, and therefore would be ruled out by the clear evidence for $g - r$ color change observed in ZTF19aatubsj.

4.4.6. The SMBH Binary Scenario

Variability on the timescales of years due to a binary SMBHB system would require a subparsec separation (e.g. Graham et al. 2015). In such a system, two SMBHBs induce tidal torques carving out a cavity in the circumbinary accretion disk, and may be surrounded by their own minidisks at sufficient separations. The interaction of accretion streams with the cavity could cause an outburst on the approximate timescales seen in this sample, which is dependent on the properties of the system. This phenomenon is seen in simulations of SMBH binaries (e.g. Ryan & MacFadyen 2017; Gold 2019).

We see evidence of offset narrow Balmer emission lines in the spectra of ZTF19aatubsj and ZTF19aaiqmgl, which may indicate a significant separate physical component, although it is unclear what is contributing to those blueshifted velocities.

5. CONCLUSIONS

We report five nuclear flaring events associated with NLSy1s, all serendipitously¹² discovered in ZTF. We measured their photometric characteristics (such as light curve shape, $g - r$ color, and rise to peak luminosity, finding a correlation between rise time and absolute magnitude), and spectroscopic properties. We then established groupings of the objects in the sample based on analyses of the months-long follow-up campaigns of these objects. Based on observed groupings of the sample, we propose the following naming scheme of spectroscopic classes of such transients for use in future optical surveys: “NLSy1-HeII”, “NLSy1-HeII+NIII”, and “NLSy1-FeII”. We ruled out the possibility that these are Type II_n supernovae occurring in NLSy1 systems. Despite the heterogeneity of the sample’s properties, two of the flares presented in this work have multiwavelength characteristics which could be consistent with TDEs in NLSy1s (ZTF19aatubsj and ZTF18abjkeo), with spectral classes of NLSy1-FeII and NLSy1-HeII, respectively. This is a high TDE rate relative to quiescent galaxies, which are more abundant than NLSy1s. The prevalence of TDE candidates in the NLSy1 AGN class could be a natural result of their hosting smaller black holes compared to typical broad-line AGN, and therefore satisfying the Hills mass criterion for an observable TDE. However, without pre-event spectra and X-ray imaging to isolate the contribution of the putative TDE to the composite NLSy1+TDE emission, flaring due to extreme AGN variability cannot be definitively ruled out. For two in the sample (ZTF19abvgxrx and ZTF19aaiqmg), we can rule out the simple TDE scenario from rebrightening in their light curves, and we determine that they, along with ZTF19aailpwl (which had a pre-flare NLSy1 spectral classification and a black hole mass estimate too large to host a canonical TDE), are likely outbursts related to enhanced accretion in excess of typical AGN variability, and with spectral features we classify as “NLSy1-HeII+NIII”, and members of the [Trakhtenbrot et al. \(2019a\)](#) class of AGN flares.

Given this sample, together with the growing number of interesting rapid optical transients associated with NLSy1s we reviewed in the literature, we posed the question of why such environments are observed to preferentially host these outbursts. Given the relative fraction of NLSy1s found with respect to other AGN classes in spectroscopic surveys such as SDSS (~15%; e.g. [Zhou et al. 2006](#); [Rakshit et al. 2017](#)), there is likely an underlying factor enhancing this rate. We suggest four different possible explanations for this enhancement:

1. A selection bias due to shorter timescales for lower mass BH systems (like NLSy1s), which are therefore more likely to be captured within the baseline of wide field optical surveys,
2. A systematic disregard of smooth flares in broad line AGN during transient searches, or
3. A true intrinsic rate enhancement due to instabilities causing rapid changes in the observable environments or accretion efficiencies of these systems.

Follow-up strategies of optical transients in AGN that are similarly ambiguous at early times may stand to benefit from the framework we offer here. We hope this classification scheme will guide real-time predictions for potential future behavior of large amplitude flares in NLSy1s, which are clearly an interesting population for future study. The next step will be to perform a systematic study of the variability of NLSy1s detected in ZTF, to assess the completeness and rate of this sample of transients with smoothly flaring light curves, and compare to a sample of broad-line AGN. Expanding on the small number of unusual transients associated with NLSy1s not only sheds light on the parameter space in which they reside, but also provides the framework for a decision tree for understanding such outbursts when they are inevitably captured at higher rates in upcoming wide field surveys. This will be imperative to establish in advance of larger and deeper surveys such as ZTF Phase II and the Vera C. Rubin Observatory (formerly known as LSST; [Ivezić et al. 2019](#)), to which the timescales of these flares are well-suited. Continued multiwavelength monitoring of the entire sample will be important to determine the host properties for those with sparse data prior to the transient, and for understanding the evolution and nature of these flares.

¹² As the [Trakhtenbrot et al. \(2019a\)](#) observational class was established midway through the ZTF survey, we had not been systematically filtering such events when the population became apparent in the nuclear transients alert stream search.

ACKNOWLEDGMENTS

We would like to thank A. Dittman for useful comments. S. Gezari is supported in part by NSF CAREER grant 1454816. We thank C. Barbarino for reducing the Nordic Optical Telescope observation of ZTF19aatubsj. We thank R. Foley for contributing the Lick Shane Kast observation of ZTF19abvgxqr. Based on observations obtained with the Samuel Oschin Telescope 48-inch and the 60-inch Telescope at the Palomar Observatory as part of the Zwicky Transient Facility project. ZTF is supported by the National Science Foundation under Grant No. AST-1440341 and a collaboration including Caltech, IPAC, the Weizmann Institute for Science, the Oskar Klein Center at Stockholm University, the University of Maryland, the University of Washington, Deutsches Elektronen-Synchrotron and Humboldt University, Los Alamos National Laboratories, the TANGO Consortium of Taiwan, the University of Wisconsin at Milwaukee, and Lawrence Berkeley National Laboratories. Operations are conducted by COO, IPAC, and UW. This work was supported by the GROWTH project funded by the National Science Foundation under Grant No 1545949. The SED Machine is based upon work supported by the National Science Foundation under Grant No. 1106171. The ZTF forced-photometry service was funded under the Heising-Simons Foundation Grant No. 12540303 (PI: Graham). These results made use of the Discovery Channel Telescope at Lowell Observatory. Lowell is a private, non-profit institution dedicated to astrophysical research and public appreciation of astronomy and operates the DCT in partnership with Boston University, the University of Maryland, the University of Toledo, Northern Arizona University and Yale University. The upgrade of the DeVeny optical spectrograph has been funded by a generous grant from John and Ginger Giovale. Based on observations made with the Nordic Optical Telescope, owned in collaboration by the University of Turku and Aarhus University, and operated jointly by Aarhus University, the University of Turku and the University of Oslo, representing Denmark, Finland and Norway, the University of Iceland and Stockholm University at the Observatorio del Roque de los Muchachos, La Palma, Spain, of the Instituto de Astrofísica de Canarias. This research has made use of data obtained through the High Energy Astrophysics Science Archive Research Center Online Service, provided by the NASA/Goddard Space Flight Center. We acknowledge the use of public data from the *Swift* data archive.

Facilities: PO:1.2m, PO:1.5m, Hale, Swift(XRT and UVOT), DCT, NOT, Shane, Liverpool:2m

Software: Pyraf,Lmfit,HEAsoft,PIMMS

REFERENCES

- Abolfathi, B., Aguado, D. S., Aguilar, G., et al. 2018, *ApJS*, 235, 42, doi: [10.3847/1538-4365/aa9e8a](https://doi.org/10.3847/1538-4365/aa9e8a)
- Ai, Y. L., Yuan, W., Zhou, H. Y., et al. 2010, *ApJL*, 716, L31, doi: [10.1088/2041-8205/716/1/L31](https://doi.org/10.1088/2041-8205/716/1/L31)
- Arcavi, I., Trakhtenbrot, B., & Hiramatsu, D. 2019, *Transient Name Server AstroNote*, 4, 1
- Assef, R. J., Stern, D., Kochanek, C. S., et al. 2013, *ApJ*, 772, 26, doi: [10.1088/0004-637X/772/1/26](https://doi.org/10.1088/0004-637X/772/1/26)
- Baldi, R. D., Capetti, A., Robinson, A., Laor, A., & Behar, E. 2016, *MNRAS*, 458, L69, doi: [10.1093/mnrasl/slw019](https://doi.org/10.1093/mnrasl/slw019)
- Barth, A. J., Pancoast, A., Bannert, V. N., et al. 2013, *ApJ*, 769, 128, doi: [10.1088/0004-637X/769/2/128](https://doi.org/10.1088/0004-637X/769/2/128)
- Bellm, E. C., Kulkarni, S. R., Graham, M. J., et al. 2019a, *PASP*, 131, 018002, doi: [10.1088/1538-3873/aaecbe](https://doi.org/10.1088/1538-3873/aaecbe)
- Bellm, E. C., Kulkarni, S. R., Barlow, T., et al. 2019b, *Publications of the Astronomical Society of the Pacific*, 131, 068003, doi: [10.1088/1538-3873/ab0c2a](https://doi.org/10.1088/1538-3873/ab0c2a)
- Bianchi, L., Shiao, B., & Thilker, D. 2017, *ApJS*, 230, 24, doi: [10.3847/1538-4365/aa7053](https://doi.org/10.3847/1538-4365/aa7053)
- Blagorodnova, N., Neill, J. D., Walters, R., et al. 2018, *PASP*, 130, 035003, doi: [10.1088/1538-3873/aaa53f](https://doi.org/10.1088/1538-3873/aaa53f)
- Blagorodnova, N., Cenko, S. B., Kulkarni, S. R., et al. 2019, *ApJ*, 873, 92, doi: [10.3847/1538-4357/ab04b0](https://doi.org/10.3847/1538-4357/ab04b0)
- Blanchard, P. K., Nicholl, M., Berger, E., et al. 2017, *ApJ*, 843, 106, doi: [10.3847/1538-4357/aa77f7](https://doi.org/10.3847/1538-4357/aa77f7)
- Boller, T., Brandt, W. N., & Fink, H. 1996, *A&A*, 305, 53
- Bruch, R. J., Gal-Yam, A., Schulze, S., et al. 2020, *arXiv e-prints*, arXiv:2008.09986. <https://arxiv.org/abs/2008.09986>
- Cappelluti, N., Predehl, P., Böhringer, H., et al. 2011, *Memorie della Societa Astronomica Italiana Supplementi*, 17, 159. <https://arxiv.org/abs/1004.5219>
- Chambers, K. C., Magnier, E. A., Metcalfe, N., et al. 2016, *arXiv e-prints*, arXiv:1612.05560. <https://arxiv.org/abs/1612.05560>
- Chan, C.-H., Piran, T., & Krolik, J. H. 2020, *arXiv e-prints*, arXiv:2004.06234. <https://arxiv.org/abs/2004.06234>
- Chan, C.-H., Piran, T., Krolik, J. H., & Saban, D. 2019, *ApJ*, 881, 113, doi: [10.3847/1538-4357/ab2b40](https://doi.org/10.3847/1538-4357/ab2b40)
- Chen, P. S., Liu, J. Y., & Shan, H. G. 2017, *NewA*, 54, 30, doi: [10.1016/j.newast.2017.01.005](https://doi.org/10.1016/j.newast.2017.01.005)
- Decarli, R., Labita, M., Treves, A., & Falomo, R. 2008, *MNRAS*, 387, 1237, doi: [10.1111/j.1365-2966.2008.13320.x](https://doi.org/10.1111/j.1365-2966.2008.13320.x)
- Drake, A. J., Djorgovski, S. G., Mahabal, A., et al. 2009, *ApJ*, 696, 870, doi: [10.1088/0004-637X/696/1/870](https://doi.org/10.1088/0004-637X/696/1/870)
- . 2011, *ApJ*, 735, 106, doi: [10.1088/0004-637X/735/2/106](https://doi.org/10.1088/0004-637X/735/2/106)
- Forster, K., & Halpern, J. P. 1996, *ApJ*, 468, 565, doi: [10.1086/177715](https://doi.org/10.1086/177715)
- Frederick, S., Kara, E., Reynolds, C., Pinto, C., & Fabian, A. 2018, *ApJ*, 867, 67, doi: [10.3847/1538-4357/aae306](https://doi.org/10.3847/1538-4357/aae306)
- Frederick, S., Gezari, S., Graham, M. J., et al. 2019, *ApJ*, 883, 31, doi: [10.3847/1538-4357/ab3a38](https://doi.org/10.3847/1538-4357/ab3a38)
- Gallegos-Garcia, M., Law-Smith, J., & Ramirez-Ruiz, E. 2018, *ApJ*, 857, 109, doi: [10.3847/1538-4357/aab5b8](https://doi.org/10.3847/1538-4357/aab5b8)
- Gallo, L. C. 2006, *MNRAS*, 368, 479, doi: [10.1111/j.1365-2966.2006.10137.x](https://doi.org/10.1111/j.1365-2966.2006.10137.x)
- Gehrels, N., Chincarini, G., Giommi, P., et al. 2004, *ApJ*, 611, 1005, doi: [10.1086/422091](https://doi.org/10.1086/422091)
- Gezari, S., van Velzen, S., Perley, D., et al. 2019, *The Astronomer's Telegram*, 13127, 1
- Gezari, S., Chornock, R., Rest, A., et al. 2012, *Nature*, 485, 217, doi: [10.1038/nature10990](https://doi.org/10.1038/nature10990)
- Gold. 2019, *Galaxies*, 7, 63, doi: [10.3390/galaxies7020063](https://doi.org/10.3390/galaxies7020063)
- Graham, M. J., Djorgovski, S. G., Drake, A. J., et al. 2017, *MNRAS*, 470, 4112, doi: [10.1093/mnras/stx1456](https://doi.org/10.1093/mnras/stx1456)
- Graham, M. J., Djorgovski, S. G., Stern, D., et al. 2015, *MNRAS*, 453, 1562, doi: [10.1093/mnras/stv1726](https://doi.org/10.1093/mnras/stv1726)
- Graham, M. J., Kulkarni, S. R., Bellm, E. C., et al. 2019, *Publications of the Astronomical Society of the Pacific*, 131, 078001, doi: [10.1088/1538-3873/ab006c](https://doi.org/10.1088/1538-3873/ab006c)
- Graham, M. J., Ross, N. P., Stern, D., et al. 2020, *MNRAS*, 491, 4925, doi: [10.1093/mnras/stz3244](https://doi.org/10.1093/mnras/stz3244)
- Gromadzki, M., Hamanowicz, A., Wyrzykowski, L., et al. 2019, *A&A*, 622, L2, doi: [10.1051/0004-6361/201833682](https://doi.org/10.1051/0004-6361/201833682)
- Grupe, D., Komossa, S., Leighly, K. M., & Page, K. L. 2010, *ApJS*, 187, 64, doi: [10.1088/0067-0049/187/1/64](https://doi.org/10.1088/0067-0049/187/1/64)
- Guainazzi, M., Nicastro, F., Fiore, F., et al. 1998, *MNRAS*, 301, L1, doi: [10.1046/j.1365-8711.1998.02089.x](https://doi.org/10.1046/j.1365-8711.1998.02089.x)
- Hawkins, M. R. S. 1998, *A&A*, 340, L23. <https://arxiv.org/abs/astro-ph/9810337>
- . 2004, *Baltic Astronomy*, 13, 642
- Hills, J. G. 1975, *Nature*, 254, 295, doi: [10.1038/254295a0](https://doi.org/10.1038/254295a0)
- Ivezić, Ž., Kahn, S. M., Tyson, J. A., et al. 2019, *ApJ*, 873, 111, doi: [10.3847/1538-4357/ab042c](https://doi.org/10.3847/1538-4357/ab042c)
- Jayasinghe, T., Stanek, K. Z., Kochanek, C. S., et al. 2019, *MNRAS*, 485, 961, doi: [10.1093/mnras/stz444](https://doi.org/10.1093/mnras/stz444)
- Kara, E., Pasham, D., Gendreau, K., & Arzoumanian, Z. 2019, *The Astronomer's Telegram*, 13132, 1
- Kasliwal, M. M., Cannella, C., Bagdasaryan, A., et al. 2019, *PASP*, 131, 038003, doi: [10.1088/1538-3873/aafbc2](https://doi.org/10.1088/1538-3873/aafbc2)
- Khazov, D., Yaron, O., Gal-Yam, A., et al. 2016, *ApJ*, 818, 3, doi: [10.3847/0004-637X/818/1/3](https://doi.org/10.3847/0004-637X/818/1/3)
- Kiewe, M., Gal-Yam, A., Arcavi, I., et al. 2012, *ApJ*, 744, 10, doi: [10.1088/0004-637X/744/1/10](https://doi.org/10.1088/0004-637X/744/1/10)
- Klimek, E. S., Gaskell, C. M., & Hedrick, C. H. 2004, *ApJ*, 609, 69, doi: [10.1086/420809](https://doi.org/10.1086/420809)

- Kochanek, C. S. 2016, *MNRAS*, 458, 127, doi: [10.1093/mnras/stw267](https://doi.org/10.1093/mnras/stw267)
- LaMassa, S. M., Cales, S., Moran, E. C., et al. 2015, *ApJ*, 800, 144, doi: [10.1088/0004-637X/800/2/144](https://doi.org/10.1088/0004-637X/800/2/144)
- Lawrence, A., Gezari, S., Elvis, M., et al. 2012, *EPJ Web of Conferences*, 39, doi: [10.1051/epjconf/20123903002](https://doi.org/10.1051/epjconf/20123903002)
- Liu, H.-Y., Yuan, W., Dong, X.-B., Zhou, H., & Liu, W.-J. 2018a, *ApJS*, 235, 40, doi: [10.3847/1538-4365/aab88e](https://doi.org/10.3847/1538-4365/aab88e)
- Liu, X., Dittmann, A., Shen, Y., & Jiang, L. 2018b, *ApJ*, 859, 8, doi: [10.3847/1538-4357/aabb04](https://doi.org/10.3847/1538-4357/aabb04)
- Liu, Z., Li, D., Liu, H.-Y., et al. 2020, *ApJ*, 894, 93, doi: [10.3847/1538-4357/ab880f](https://doi.org/10.3847/1538-4357/ab880f)
- Lunnan, R., Yan, L., Perley, D. A., et al. 2019, arXiv e-prints, arXiv:1910.02968. <https://arxiv.org/abs/1910.02968>
- MacLeod, C. L., Ross, N. P., Lawrence, A., et al. 2016, *MNRAS*, 457, 389, doi: [10.1093/mnras/stv2997](https://doi.org/10.1093/mnras/stv2997)
- Malyali, A., Rau, A., Arcodia, R., et al. 2020, *The Astronomer's Telegram*, 13712, 1
- Marconi, A., Axon, D. J., Maiolino, R., et al. 2008, *ApJ*, 678, 693, doi: [10.1086/529360](https://doi.org/10.1086/529360)
- Masci, F. J., Laher, R. R., Rusholme, B., et al. 2019, *PASP*, 131, 018003, doi: [10.1088/1538-3873/aae8ac](https://doi.org/10.1088/1538-3873/aae8ac)
- Mathur, S., Aucht, K., Kochanek, C. S., et al. 2019, *The Astronomer's Telegram*, 13213, 1
- Mathur, S., Kuraskiewicz, J., & Czerny, B. 2001, *NewA*, 6, 321, doi: [10.1016/S1384-1076\(01\)00058-6](https://doi.org/10.1016/S1384-1076(01)00058-6)
- McLure, R. J., & Dunlop, J. S. 2002, *MNRAS*, 331, 795, doi: [10.1046/j.1365-8711.2002.05236.x](https://doi.org/10.1046/j.1365-8711.2002.05236.x)
- Merloni, A., Dwelly, T., Salvato, M., et al. 2015, *MNRAS*, 452, 69, doi: [10.1093/mnras/stv1095](https://doi.org/10.1093/mnras/stv1095)
- Meusinger, H., Henze, M., Birkle, K., et al. 2010, *A&A*, 512, A1, doi: [10.1051/0004-6361/200913526](https://doi.org/10.1051/0004-6361/200913526)
- Miller, H. R., Ferrara, E. C., McFarland, J. P., et al. 2000, *NewAR*, 44, 539, doi: [10.1016/S1387-6473\(00\)00094-4](https://doi.org/10.1016/S1387-6473(00)00094-4)
- Miller, J. M., Zoghbi, A., Reynolds, M., et al. 2019, *The Astronomer's Telegram*, 13163, 1
- Molthagen, K., Bade, N., & Wendker, H. J. 1998, *A&A*, 331, 925
- Moriya, T. J., Sorokina, E. I., & Chevalier, R. A. 2018, *SSRv*, 214, 59, doi: [10.1007/s11214-018-0493-6](https://doi.org/10.1007/s11214-018-0493-6)
- Neustadt, J. M. M., Holoiu, T. W. S., Kochanek, C. S., et al. 2020, *MNRAS*, 494, 2538, doi: [10.1093/mnras/staa859](https://doi.org/10.1093/mnras/staa859)
- Nikołajuk, M., Czerny, B., & Gurynowicz, P. 2009, *MNRAS*, 394, 2141, doi: [10.1111/j.1365-2966.2009.14478.x](https://doi.org/10.1111/j.1365-2966.2009.14478.x)
- Nordin, J., Brinnel, V., van Santen, J., et al. 2019, *A&A*, 631, A147, doi: [10.1051/0004-6361/201935634](https://doi.org/10.1051/0004-6361/201935634)
- Pasham, D., Gendreau, K., Arzoumanian, Z., et al. 2020, *The Astronomer's Telegram*, 14036, 1
- Patterson, M. T., Bellm, E. C., Rusholme, B., et al. 2019, *PASP*, 131, 018001, doi: [10.1088/1538-3873/aae904](https://doi.org/10.1088/1538-3873/aae904)
- Payne, A. V., Shappee, B. J., Hinkle, J. T., et al. 2020, arXiv e-prints, arXiv:2009.03321. <https://arxiv.org/abs/2009.03321>
- Pogge, R. W. 2000, *NewAR*, 44, 381, doi: [10.1016/S1387-6473\(00\)00065-8](https://doi.org/10.1016/S1387-6473(00)00065-8)
- Pounds, K. A., Done, C., & Osborne, J. P. 1995, *MNRAS*, 277, L5, doi: [10.1093/mnras/277.1.L5](https://doi.org/10.1093/mnras/277.1.L5)
- Rafter, S. E., Kaspi, S., Chelouche, D., et al. 2013, *ApJ*, 773, 24, doi: [10.1088/0004-637X/773/1/24](https://doi.org/10.1088/0004-637X/773/1/24)
- Rakshit, S., Stalin, C. S., Chand, H., & Zhang, X.-G. 2017, *The Astrophysical Journal Supplement Series*, 229, 39, doi: [10.3847/1538-4365/aa6971](https://doi.org/10.3847/1538-4365/aa6971)
- Rigault, M., Neill, J. D., Blagorodnova, N., et al. 2019, *A&A*, 627, A115, doi: [10.1051/0004-6361/201935344](https://doi.org/10.1051/0004-6361/201935344)
- Ross, N. P., Ford, K. E. S., Graham, M., et al. 2018, *MNRAS*, 480, 4468, doi: [10.1093/mnras/sty2002](https://doi.org/10.1093/mnras/sty2002)
- Ruan, J. J., Anderson, S. F., Cales, S. L., et al. 2016, *ApJ*, 826, 188, doi: [10.3847/0004-637X/826/2/188](https://doi.org/10.3847/0004-637X/826/2/188)
- Runnoe, J. C., Cales, S., Ruan, J. J., et al. 2016, *MNRAS*, 455, 1691, doi: [10.1093/mnras/stv2385](https://doi.org/10.1093/mnras/stv2385)
- Ryan, G., & MacFadyen, A. 2017, *ApJ*, 835, 199, doi: [10.3847/1538-4357/835/2/199](https://doi.org/10.3847/1538-4357/835/2/199)
- Saxton, C. J., Perets, H. B., & Baskin, A. 2018, *MNRAS*, 474, 3307, doi: [10.1093/mnras/stx2928](https://doi.org/10.1093/mnras/stx2928)
- Schmidt, R. W., & Wambsganss, J. 2010, *General Relativity and Gravitation*, 42, 2127, doi: [10.1007/s10714-010-0956-x](https://doi.org/10.1007/s10714-010-0956-x)
- Shen, Y., Richards, G. T., Strauss, M. A., et al. 2011, *ApJS*, 194, 45, doi: [10.1088/0067-0049/194/2/45](https://doi.org/10.1088/0067-0049/194/2/45)
- Smartt, S. J., Smith, K. W., McBrien, O., et al. 2019, *Transient Name Server AstroNote*, 33, 1
- Sollerman, J., Taddia, F., Arcavi, I., et al. 2019, *A&A*, 621, A30, doi: [10.1051/0004-6361/201833689](https://doi.org/10.1051/0004-6361/201833689)
- Sollerman, J., Fransson, C., Barbarino, C., et al. 2020, arXiv e-prints, arXiv:2009.04154. <https://arxiv.org/abs/2009.04154>
- Soumagnac, M. T., & Ofek, E. O. 2018, *PASP*, 130, 075002, doi: [10.1088/1538-3873/aac410](https://doi.org/10.1088/1538-3873/aac410)
- Stein, R., van Velzen, S., Kowalski, M., et al. 2020, arXiv e-prints, arXiv:2005.05340. <https://arxiv.org/abs/2005.05340>
- Stern, D., Assef, R. J., Benford, D. J., et al. 2012, *ApJ*, 753, 30, doi: [10.1088/0004-637X/753/1/30](https://doi.org/10.1088/0004-637X/753/1/30)
- Stern, D., McKernan, B., Graham, M. J., et al. 2018, *ApJ*, 864, 27, doi: [10.3847/1538-4357/aac726](https://doi.org/10.3847/1538-4357/aac726)

- Tadhunter, C., Spence, R., Rose, M., Mullaney, J., & Crowther, P. 2017, *Nature Astronomy*, 1, 0061, doi: [10.1038/s41550-017-0061](https://doi.org/10.1038/s41550-017-0061)
- Tananbaum, H., Avni, Y., Branduardi, G., et al. 1979, *ApJL*, 234, L9, doi: [10.1086/183100](https://doi.org/10.1086/183100)
- Terlevich, R., Tenorio-Tagle, G., Franco, J., & Melnick, J. 1992, *MNRAS*, 255, 713, doi: [10.1093/mnras/255.4.713](https://doi.org/10.1093/mnras/255.4.713)
- Trakhtenbrot, B., Arcavi, I., Ricci, C., & Burke, J. 2020, *Transient Name Server AstroNote*, 105, 1
- Trakhtenbrot, B., Arcavi, I., Ricci, C., et al. 2019a, *Nature Astronomy*, 3, 242, doi: [10.1038/s41550-018-0661-3](https://doi.org/10.1038/s41550-018-0661-3)
- Trakhtenbrot, B., Arcavi, I., MacLeod, C. L., et al. 2019b, arXiv e-prints, arXiv:1903.11084. <https://arxiv.org/abs/1903.11084>
- Uttley, P., McHardy, I. M., Papadakis, I. E., Guainazzi, M., & Fruscione, A. 1999, *MNRAS*, 307, L6, doi: [10.1046/j.1365-8711.1999.02801.x](https://doi.org/10.1046/j.1365-8711.1999.02801.x)
- van Velzen, S., Holoien, T. W. S., Onori, F., Hung, T., & Arcavi, I. 2020a, arXiv e-prints, arXiv:2008.05461. <https://arxiv.org/abs/2008.05461>
- van Velzen, S., Mendez, A. J., Krolik, J. H., & Gorjian, V. 2016, *ApJ*, 829, 19, doi: [10.3847/0004-637X/829/1/19](https://doi.org/10.3847/0004-637X/829/1/19)
- van Velzen, S., Gezari, S., Cenko, S. B., et al. 2019, *ApJ*, 872, 198, doi: [10.3847/1538-4357/aafe0c](https://doi.org/10.3847/1538-4357/aafe0c)
- van Velzen, S., Gezari, S., Hammerstein, E., et al. 2020b, arXiv e-prints, arXiv:2001.01409. <https://arxiv.org/abs/2001.01409>
- Wang, T., Brinkmann, W., & Bergeron, J. 1996, *A&A*, 309, 81
- Wevers, T., Pasham, D. R., van Velzen, S., et al. 2019, *MNRAS*, 488, 4816, doi: [10.1093/mnras/stz1976](https://doi.org/10.1093/mnras/stz1976)
- Xu, D., Komossa, S., Zhou, H., et al. 2012, *AJ*, 143, 83, doi: [10.1088/0004-6256/143/4/83](https://doi.org/10.1088/0004-6256/143/4/83)
- Yan, L., Wang, T., Jiang, N., et al. 2019, *ApJ*, 874, 44, doi: [10.3847/1538-4357/ab074b](https://doi.org/10.3847/1538-4357/ab074b)
- Yan, L., Perley, D., Schulze, S., et al. 2020, arXiv e-prints, arXiv:2006.13758. <https://arxiv.org/abs/2006.13758>
- Zhou, H., Wang, T., Yuan, W., et al. 2006, *ApJS*, 166, 128, doi: [10.1086/504869](https://doi.org/10.1086/504869)

APPENDIX

The light curves in Figure 10 are from the second IPAC data release of ZTF forced photometry. Figure 11 shows the region of interest around He II, $H\beta+[O III]$, and the Fe II complex for all follow-up spectra taken of the sample.

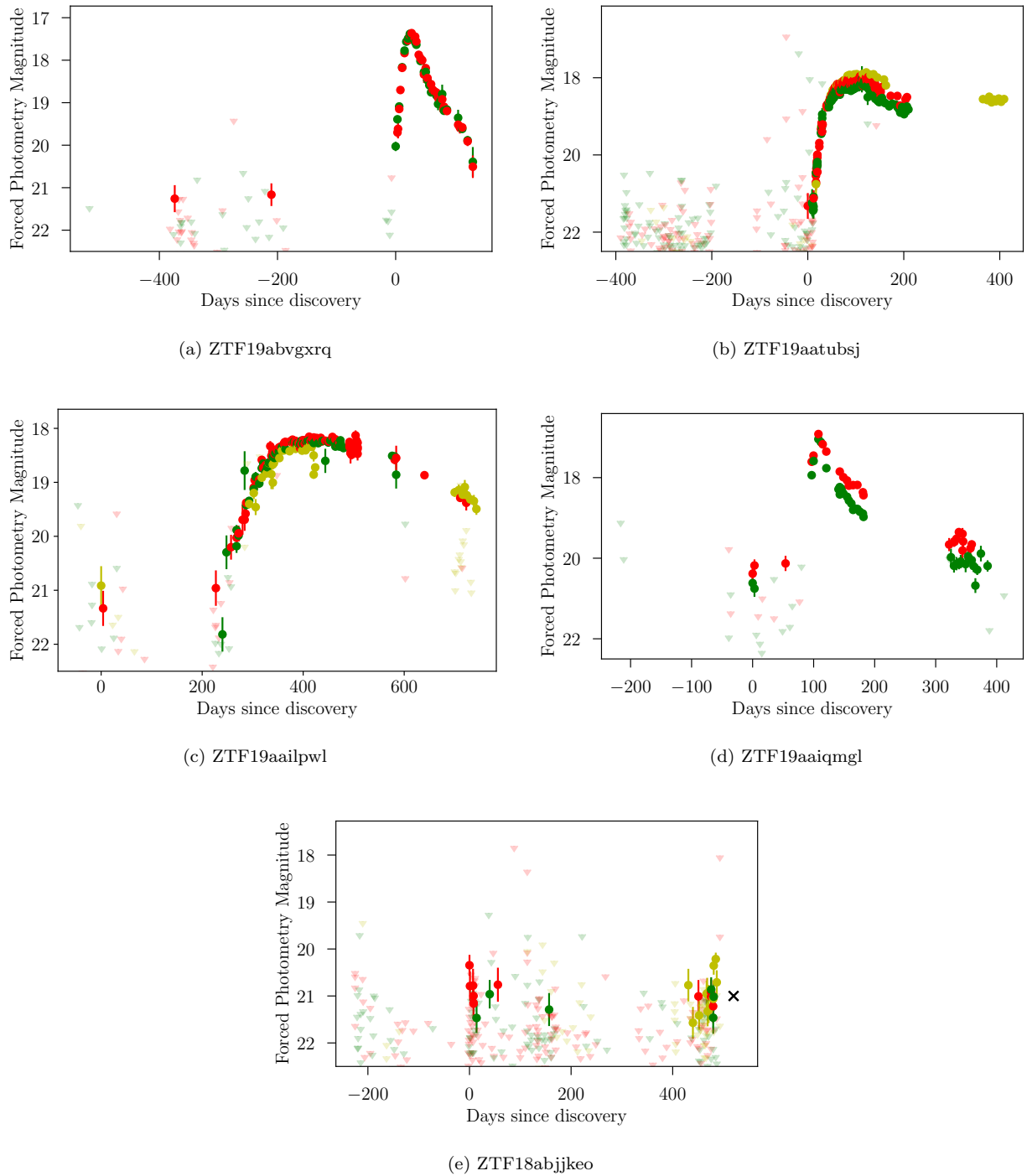


Figure 10. Forced photometry of the sample from ZTF Data Release 3. Colors correspond to r -, g -, and i -band $3\text{-}\sigma$ detections, and triangles correspond to $5\text{-}\sigma$ upper limits. An ‘X’ marks the rise to peak in the difference imaging light curve of ZTF18abjjkeo, which was discovered in data too recent to be included in the ZTF DR3, and therefore only shows the flux level of the host galaxy. The data points in the light curves beyond 2020 will be released in the final ZTF photometry data release.

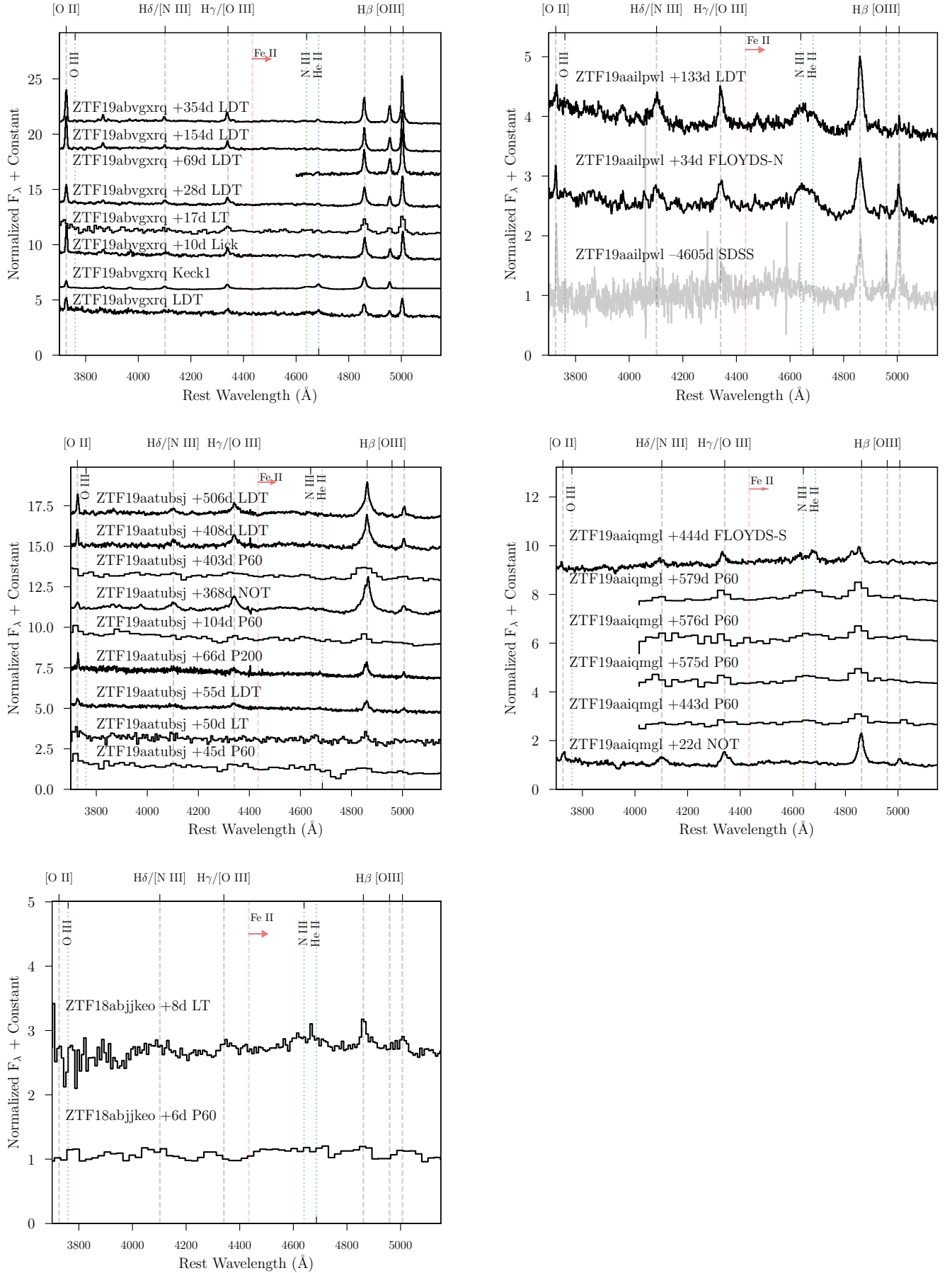


Figure 11. Spectroscopic follow-up of the sample summarized in Table 1, showing the evolution of the He II, H β , and Fe II line complexes.